

AN ANALOG COMPUTER FOR THE SOLUTION OF  
EIGENVALUE PROBLEMS

Thesis by  
George Jay Gleghorn, Jr.

In Partial Fulfillment of the Requirements  
for the Degree of  
Doctor of Philosophy

California Institute of Technology  
Pasadena, California

1955

#### ACKNOWLEDGEMENT

The writer wishes to express his sincere appreciation to various members of the California Institute of Technology Staff with whom he has been associated in the course of his graduate work. He wishes particularly to thank Dr. R. H. MacNeal, who directed the research, for the many valuable suggestions and criticisms which he made.

The writer is indebted to the Engineering Department of the Institute, which sponsored the construction of the computer.

The writer is appreciative of the work of Joyce Martin, who prepared the final copy of the thesis. He is especially grateful to his wife, Barbara, for typing the rough draft, and for her continued help and encouragement.

## ABSTRACT

This thesis describes a computer suitable for the determination of the eigenvalues and eigenvectors of conservative mechanical and electrical systems.

In essence, the computer consists of several active circuits with input impedances which act as negative resistances at the operating frequency of the computer. These negative resistances are interconnected with passive resistors and transformers to form a circuit analogous to the system being studied. For any setting of the control the analog represents the original system at a single frequency only, consequently it cannot be used for transient analysis.

It is shown that the analog circuit is, in general, unstable at the control settings that are of interest, but that the application of suitable constraints suppresses the oscillations so that measurements may be made. The negative resistance circuits are designed so that parasitic impedances have little effect on the results. The computer has been found to produce results accurate to one per cent in most cases.

## TABLE OF CONTENTS

PART	TITLE	PAGE
I.	Introduction	1
II.	Properties of Eigenvalues and Eigenvectors	3
	2.1 Conservative Mechanical System	3
	2.2 Properties of the Eigenvalues	6
	2.3 Nodes - Some Properties of Eigenvectors	7
III.	Theory and Methods of Operation	9
	3.1 Analogous Systems	9
	3.2 Single Frequency Analogy	10
	3.3 Instability of the Analog	11
	3.4 Determination of Eigenvalues and Eigenvectors	15
IV.	Construction of the Computer	22
	4.1 Primary Considerations	22
	4.2 Negative Conductance Generators	23
	4.3 R-C Coupled Feedback Amplifiers	27
	4.4 D. C. Amplifiers	31
	4.5 Dual Locus Nyquist Diagrams	31
	4.6 Effect of Parasitic Impedances	34
	4.7 Generator Frequency Response Requirements	37
	4.8 Test Results	39
V.	Results of Tests on Analogs	53
	5.1 Computation of the Eigenvalues and Eigenvectors of a Simple System	53
	5.2 Example of Stationary Power Input	55
	5.3 Torsional Vibration of a Rod	56

PART	TITLE	PAGE
	5.4 Bending of a Beam	58
	5.5 Bending of a Plate	62
VI.	Discussion and Conclusion	74
	References	76
	Appendix I	78

## I. INTRODUCTION

In recent years lumped electrical analogs of many continuous systems have been developed, intended primarily for the study of large scale systems by electric analog computers. Of particular interest are electrical analogs for wave equation vibration problems as typified by the vibrating string or membrane, (Refs. 1, 2) and for the bending of beams, plates and other structural members (Refs. 3, 4, 5). In most cases the physical systems are conservative and the analogs employ only reactive elements.

In the solution of potential problems, on the other hand, use of resistance networks (Ref. 6) allows highly accurate solutions to be obtained at a relatively low cost. Elaborating on this approach, Swenson (Refs. 7, 8, 9) has developed a direct current computer for solution of membrane vibration problems. This computer consists of a large number of resistors arranged in a grid to represent the tension in the membrane and of several active circuits which serve as negative resistances to represent the mass. In operation these negative resistances are set to values corresponding to a given vibration frequency and the circuits are then successively balanced by hand, several balancing operations usually being required due to the coupling involved.

In working with this computer Swenson found that the lowest mode could be easily obtained while driving the system at one point and observing the vibration frequency corresponding to zero input admittance. Higher modes could be obtained only when the position of their nodal lines were known, thus reducing the problem to finding the lowest mode of a smaller region. He noted that it was impossible to obtain a balanced condition in any network when the vibration frequency was set to a value

higher than the frequency at which the input admittance became infinite.

The present work extends that of Swenson in two ways: the problem of hand balancing the negative resistors is eliminated by the use of self-balancing feed back circuits and modes other than the lowest are obtained directly by employing multiple constraints or driving points. In addition alternating current is used for computation, in order to handle analogs which require transformers.

Some of the basic properties of eigenvalues and eigenvectors are discussed in Part II. The relative magnitudes of eigenvalues of systems having one or more constraints is of particular importance.

Part III is an exposition of the theory of operation of the computer. It is shown that, without constraints, an analog becomes unstable at the lowest normal mode, but that it may be made stable at all modes if a sufficient number of constraints are applied. To achieve this result, it is sufficient to assume that the negative resistance circuits have identical frequency responses. Finally, various techniques of obtaining a balance with several constraints are discussed.

The actual construction of the computer is discussed in Part IV. Here various practical considerations such as impedance level, ease of operation, etc. are taken into account. In addition it is shown that operation is essentially unaffected by small departures of individual negative resistance circuits from the standard frequency response, or by parasitic reactances in the computing resistors or transformers. The results of various tests performed on the computing circuits are included.

Several examples are worked out in detail in Part V to illustrate various points and to test the accuracy of the computer. The results indicate that it is not unreasonable to expect accuracies in the order of 1% on both eigenvalues and eigenvectors.

## II. PROPERTIES OF EIGENVALUES AND EIGENVECTORS

### 2.1 Conservative Mechanical System

Consider a system of masses interconnected by springs and perhaps by levers, bars, etc., resulting in holonomic constraints\*. It will be assumed that the system is conservative. The system is said to have  $n$  degrees of freedom if the motion of the system is known when the values of  $n$  coordinates  $q_1, q_2, \dots, q_n$  are specified. The motion of such a system can be expressed by the differential equation

$$M\ddot{q} + Kq = Q_i, \quad (\text{II-1})$$

where  $M$  is the  $n \times n$  matrix

$$M = (m_{ij}) = \begin{bmatrix} m_{11} & m_{12} & \dots & m_{1n} \\ m_{21} & m_{22} & \dots & \\ \vdots & \vdots & \ddots & \\ m_{n1} & m_{n2} & \dots & m_{nn} \end{bmatrix}$$

and  $q$  is the column matrix

$$q = \{q_i\} = \begin{bmatrix} q_1 \\ q_2 \\ \vdots \\ q_n \end{bmatrix} \cdot$$

The superscript "t" will indicate the transposed matrix.

---

\* A constraint is said to be holonomic if the equation describing it involves the values of the coordinates only, or, if time derivatives of the coordinates are involved, when it can be integrated without further knowledge of the motion.



Unless otherwise indicated, it is assumed that all square matrices are symmetric and that all elements are real.

The equations of "free vibration" are obtained by setting the driving forces  $Q_i$  equal to zero. It is possible to introduce a coordinate transformation of the form  $q = A u$  which will simultaneously diagonalize both  $M$  and  $K$  (Ref 10, pg. 187). If the equations are also normalized so that  $A^t M A$  becomes the unit matrix  $E_n = (\delta_{ij})$ ,

$$A^t M A \ddot{u} + A^t K A u = 0$$

$$E_n \ddot{u} + D u = 0. \quad (\text{II-2})$$

Here  $D$  is the  $n \times n$  matrix with diagonal terms  $r_1, r_2, \dots, r_n$ ; all other terms being zero. The coordinates  $u_k$  are called the normal coordinates of the system and the  $r$ 's are the squares of the normal frequencies of vibration of the system. These numbers are often termed characteristic numbers or eigenvalues. These terms will be used interchangeably. The columns of the transformation matrix  $A$  are called the mode shapes or eigenvectors of the system, for they specify the relative magnitudes (and phases) of the displacements of the various coordinates when the system is vibrating at the appropriate normal frequency.

The usefulness of the normal mode concept comes about through use of the principle of superposition, which leads to the result that the response of the system to any arbitrary set of forces may be expressed as a linear combination of the normal vibrations. This is most easily seen, perhaps, by applying the transformation directly to the non-homogeneous equation (II-1):

$$A^t \{M A \ddot{u} + K A u\} = A^t \{Q_i\} = \{Q_k\}. \quad (\text{II-3})$$

The resulting n equations

$$\{\ddot{u}_k + \omega_k^2 u_k\} = \{Q_k(t)\} = A^t \{Q_i\}; \quad (\text{II-4})$$

may be solved for  $u_k(t)$ , the  $q_i(t)$  then being obtained by again applying the transformation. When the transformation used is one which has not been normalized, (II-4) may be written in the alternative form

$$\ddot{u}_k + \omega_k^2 u_k = \frac{A^t \{Q_i\}}{A^t M A}. \quad (\text{II-5})$$

The theory outlined above is useful from an analytical point of view and in establishing the existence of a solution, but it ignores the important point that the matrix A is unknown at the outset. There are several numerical methods which may be used to find this matrix in special cases. One such method makes use of the assumption that u is of the form  $u = \{u_k \cos(\omega t + \beta_k)\}$ . Substituting in the equation of free vibration, (II-1 with  $Q_i = 0$ ) yields a set of linear homogeneous equations

$$[-\omega^2 M + K] A \{u_k \cos(\omega t + \beta_k)\} = 0. \quad (\text{II-6})$$

These equations possess a non-trivial solution only when the determinantal equation

$$|K - \omega^2 M| = 0 \quad (\text{II-7})$$

is satisfied. Solution of the equation is obtained for n values of  $\lambda = \omega^2$  (the eigenvalues) each one of which allows one column of A to be determined from (II-7).\*

---

\* Degenerate forms occurring when two or more eigenvalues are equal are not considered here. See Ref. 1, p. 16 and Ref. 12)

## 2.2 Properties of the Eigenvalues

The eigenvalues of the system described, and of any system where the matrices M and K are real and symmetric, may be shown to be real. (Ref. 10, pg 196). Since it has also been assumed that the matrices are positive semi-definite, the eigenvalues are all of the same sign (zero included) (Ref. 10, pg 196). Unless otherwise noted, the sign will always be chosen positive. The eigenvalues may be conveniently indexed in order of magnitude:  $0 \leq \lambda_1 \leq \lambda_2 \leq \lambda_3 \dots \leq \lambda_n$ .

If the original system is subjected to r auxiliary conditions of the type  $\sum_{i=1}^n a_i q_i = 0$ , called "constraints", the number of degrees of freedom of the system is reduced and the n-r new or "constrained" eigenvalues,  $\lambda^{(r)}$ , are related to the original ones by the inequalities (Ref. 13, pg 286)

$$\lambda_k \leq \lambda_k^{(r)} \leq \lambda_{k-r} \quad . \quad (II-8)$$

In particular for one constraint

$$\lambda_1 \leq \lambda_1' \leq \lambda_2 \leq \lambda_2' \dots \leq \lambda_{n-1}' \leq \lambda_{n-1} \leq \lambda_n. \quad (II-9)$$

Constrained eigenvalues for systems with greater numbers of constraints are similarly interleaved with those for the system having one less constraint.

Two other properties of eigenvalues are of interest. As stated by Courant and Hilbert (Ref. 13, pg 286),

"As the inertia increases, the pitch of the fundamental tone and every overtone decreases (or remains the same).

If the system stiffens, the pitch of the fundamental tone and every overtone increases (or remains the same).

Increase of inertia means change to a system with kinetic energy  $T'$  such that  $T'-T$  is never negative, while the potential energy remains unchanged."

### 2.3 Nodes - Some Properties of Eigenvectors

Nodes of eigenvectors are points which are motionless when the system is vibrating in a normal mode. They are, perhaps, easiest to visualize by considering continuous systems rather than the discrete systems previously discussed. A classical example is the standing waves of a vibrating string or membrane. In the one dimensional case of the string, nodal points separate two adjacent regions vibrating with opposite phase. Similarly, nodal lines occur on the vibrating membrane. As an example of the three dimensional case, resonant cavities exhibit nodal surfaces where the electric or magnetic field intensity is zero.

In a discrete system it will be assumed that a node can exist at a mass, in which case the appropriate element of the eigenvector is zero; or at a point of a spring between two masses, in which case the elements of the eigenvector corresponding to the two masses connected are of opposite sign.

While there are many general properties of eigenvalues as described above, much less is known of the general behavior of the nodes of eigenvectors. Of course, the transformation introduced in the diagonalization of the system matrix implies that the weighted orthogonality conditions

$$\begin{aligned} A^t M A &= E_n & (II-10) \\ A^t K A &= D \end{aligned}$$

hold in all cases. It can also be shown\* that the  $h$ -th eigenvector has

---

\*Appendix I and Reference 13, pg 451.

no more than  $h-1$  nodes, and therefore no more than  $h$  subregions separated by nodes. This taken in conjunction with the orthogonality conditions shows that every subregion corresponding to a given eigenvalue must have within it a point or points corresponding to some node of each higher eigenvector. In a system with one space variable (for example where the masses can move only along a line) it can be shown that there are exactly  $h-1$  nodes of the  $h$ -th eigenvector. In particular the lowest mode of any system has no nodes. Several examples illustrating these properties may be found in Part V.

### III. THEORY AND METHODS OF OPERATION

#### 3.1 Analogous Systems

It has long been recognized (Ref. 14, Ch V) that systems of linear second-order differential equations serve to describe lumped constant electrical networks as well as mechanical systems. Two such systems are said to be analogous when they are described by identical sets of equations.

There are two commonly used electrical analogies to mechanical systems. They may conveniently be designated as the current-force and voltage-force analogies. Although electrical analogs may be developed on either basis the current-force analogy has proven most useful in analog computer study of vibrating systems and will, therefore, be the only one considered here. Corresponding quantities are listed in Table III-1, which is adapted from Gardner and Barnes (Ref. 15, Chap. II)

Table III-1

#### Corresponding Quantities in Current-Force Analogy

<u>Mechanical</u>	<u>Electrical</u>
Mass	Capacitance
Spring Compliance	Inductance
Viscous Damping	Conductance
Force	Current
Velocity	Voltage
Lever	Ideal transformer

Lumped element electrical analogs have been developed for many continuous mechanical systems by the use of finite difference techniques (Ref. 3,4) and by other methods (Ref. 16). We will be primarily concerned with such systems, and in particular with those which are conservative.

### 3.2 Single Frequency Analogy

If attention is restricted to a single frequency an electrical analog based on equation (II-1) may be used. Taking  $Q_1 = I_1 \cos \omega t$  and  $q_1 = v_1 \cos \omega t$  and restricting attention to the amplitude of the voltage and current gives

$$(-\omega^2 M + K) v = I . * \quad (III-1)$$

If the possibility of using a negative resistance is admitted, an analog can be constructed employing the following equivalent elements:

#### Mechanical

Mass (times  $\omega^2$ )  
Spring Compliance  
Viscous Damping

#### Electrical

Negative conductance  
Positive resistance  
none

It is seen, by comparing with Table III-1, that any pure reactance network can be represented, at a single frequency, by a purely resistive network with the proper values of negative and positive conductance replacing capacitance and inverse inductance respectively. It should be noted that the value of  $\omega$  in (III-1) bears no relation to the actual angular frequency of the voltage and current. It is merely a parameter used in the study of the system and affects the value of the negative conductances. In fact, if there are no transformers in the network, direct current may be used as the "working frequency".

The actual method to be used in obtaining the required negative conductances is, of course, of great importance and will be discussed in Part IV. It will be sufficient for the present, however, to assume that

---

\*To simplify the figures and equations the mechanical labeling will be used for electrical components when referring to the analogous systems. It is understood that an admittance base has been chosen for representing both mass and spring constants.

each negative conductance is replaced by a "black box" which has the input admittance  $f(p) m_{ij}$ . It is assumed that the frequency dependence of each black box is identical. This restriction will be removed in the discussion of parasitics, Section 4.6. It is seen that (III-1) in conjunction with (II-7) implies a restriction on  $f(p)$ , namely

$$f(j \omega_0) = -\lambda \quad (\text{III-2})$$

where, for generality, the eigenvalue parameter  $\lambda$  has replaced  $\omega^2$  and  $\omega_0$  is the working angular frequency.

### 3.3 Instability of the Analog

Inter-connection of many active elements always raises the possibility of instability. In the case of an analog using negative conductance generators the characteristic equation of the system is the determinantal equation

$$|K + f(p) M| = 0. \quad (\text{III-3})$$

This equation is identical with (II-7) if we replace  $\omega^2$  by  $-f(p)$ .

As pointed out in sections 2.2 and 2.3, the solutions of (II-7) and therefore of (III-3) are the eigenvalues of the system. Thus, (III-3) may be re-written as a product:

$$(f(p) - \lambda_1) (f(p) - \lambda_2) \dots (f(p) - \lambda_n) = 0. \quad (\text{III-4})$$

Now each factor may be set equal to zero and the Nyquist criterion (Ref. 17, ch VIII) may be applied to each in turn. If any factor indicates instability, the entire system is unstable. The separate plots may be combined into one, for it is seen that the system is unstable if the locus of  $f(j\omega)$  encircles any of the points  $(-\lambda_k + j0)$ .



Effects of deviations of the impedances from pure conductance, and of slight dissimilarities of the amplifiers will be discussed in Section 4.6.

It is customary to determine the normal mode frequencies of electric analogs by driving the system at one point with a variable frequency oscillator, holding the voltage constant and measuring the current entering the system. A normal mode is indicated by minimum input admittance as detected by a current null or by unity power factor, which occur at the same frequency since we are assuming no damping.

If the purely conductive analog is not driven by any external current or voltage sources, as the parameter  $\lambda$  is raised from zero to a positive value\* the voltages at all junctions remains zero until the value  $\lambda_1$  is reached, at which point the system breaks into oscillation. These oscillations will, in general, increase in magnitude until limited by the nonlinearities of the system, so that it would be useless to attempt to obtain higher modes, or even the shape of the lowest mode, without taking steps to eliminate the oscillations.\*\*

Assume, then, that one of the junctions, say the  $n$ -th, is being driven by an oscillator of low impedance and frequency  $\omega_0$ , such that

$$v_n = \frac{2p}{p^2 + \omega_0^2} \cdot$$

- 
- \* It is assumed that the  $\lambda$  of all negative conductances can be varied continuously and simultaneously.
  - \*\* It was possible by very critical adjustment of  $\lambda$  to make some systems oscillate in the lowest mode shape without saturation. However, shifting of measuring equipment from point to point altered the circuit sufficiently to disturb this condition.

(Note that there are no other voltages applied).

Equations (III-1) may be re-written as n-1 equations of the form

$$\begin{aligned} (k_{i1} + m_{i1}f(p)) v_1 + (k_{i2} + m_{i2}f(p)) v_2 \dots \\ = - \frac{(k_{in} + m_{in}f(p)) p}{p^2 + \omega_0^2} \end{aligned} \quad \text{(III-5)}$$

the n-th equation having been eliminated. This set of equations determines a new characteristic equation having a determinant which is that of the original system with one constraint. The roots of this equation are obtained for  $-f(p) = \lambda'_k$ .\* The Nyquist Diagram for this case is shown in Figure 1 for a value of  $\lambda$  lying between  $\lambda_1$  and  $\lambda'_1$ . Equation (III-2) indicated that the point  $-f(j\omega_0)$  lies on the positive real axis as shown. By (II-7) it is seen that it is always possible, in the absence of degenerate roots, to obtain the lowest mode without instability of the system by driving the system at one point, and moreover, the choice of the point is arbitrary.

It is also evident that  $\lambda$  cannot be increased indefinitely without causing instability, for eventually the plot will encircle one of the  $\lambda k'$ . Of course, by the exercise of some ingenuity it is theoretically possible to sketch a plot of  $-f(j\omega)$  which would allow stability at a higher eigenvalue while still avoiding a critical point (Fig. 2), but this would require some knowledge of the eigenvalues and would certainly not allow  $\lambda$  to be continuously variable.

Fortunately, there is another method of approach to the problem which is practicable. Consider the network with one voltage source applied. The lowest eigenvalue is the lowest one of the original system with one constraint applied. Referring to Section 2.2, if a constraint

---

\* See Section 2.2

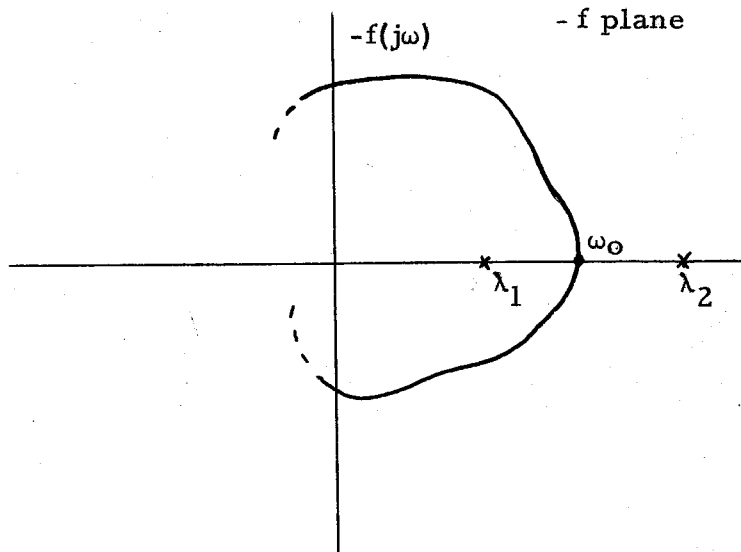


Figure 1. Nyquist Diagram Illustrating Stability at  $\lambda_1$

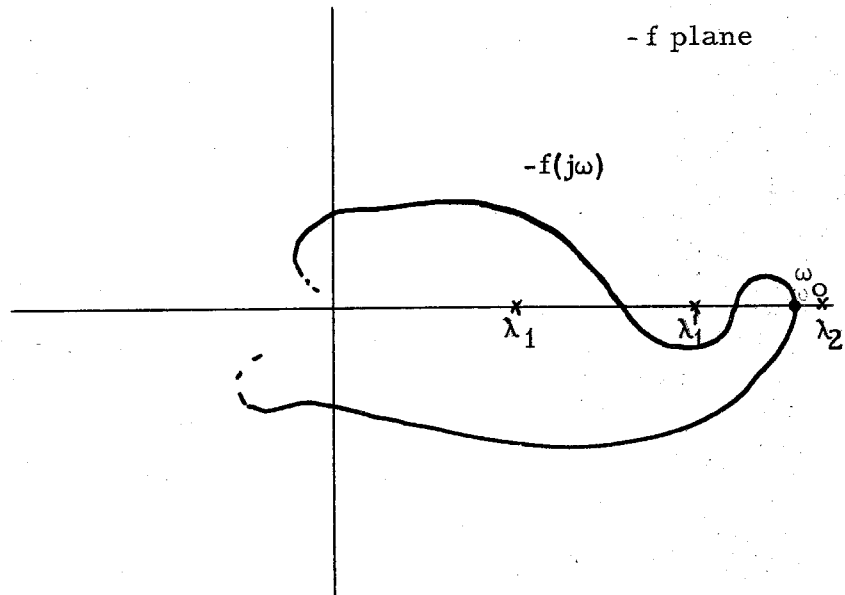


Figure 2. Nyquist Diagram - Conditional Stability Near  $\lambda'_1$

is added to a system it raises the value of the lowest eigenvalue. In order to keep the system stable in the vicinity of  $\lambda_2$ , then, additional constraints may be added until the lowest eigenvalue of the constrained system is greater than  $\lambda_2$ . Continuing the process assures stability at higher eigenvalues.

The properties of eigenvectors are outlined in Section 2.3 are useful in making a judicious choice of points at which to apply the constraints. In order for the system to be stable in the vicinity of any eigenvalue, there must at least be one constraint applied in each of the regions separated by the nodes of the eigenvector. If there is not, then the unconstrained region will oscillate, for it may be considered as a separate eigenvalue problem having a boundary of zero deflection corresponding to the node and its lowest eigenvalue will be the one sought. This also indicates that the constraints must be chosen so that there is no region with fixed boundary passing through constrained points which has a lowest eigenvalue lower than the one being sought. In this matter experience is the best teacher. The following section discusses the points in more detail.

#### 3.4 Determination of Eigenvalues and Eigenvectors

With stability of the system assured by the use of constraints, there remains the problem of determining the eigenvalues and eigenvectors of the homogeneous system. In the pure reactance analogy, the input admittance at one point is measured, the system being driven at that point only. There is, of course, only one input current. This is the situation we are trying to duplicate, but inherent instability requires that the pure conductance analogy be driven at several points. If, however, the several constraining voltages can be adjusted so as to

make all the currents in the additional or "variable" constraints zero, the current into the original driving point or "fixed" constraint is a measure of the input admittance. This current may be plotted against  $\lambda$  as an aid in finding the eigenvalues. At an eigenvalue, reducing the additional constraint currents to zero will automatically cause the current at the "fixed" constraint to be zero. The eigenvector is found by direct measurement of the voltages at the junctions when all currents are zero.

When there is only one variable constraint the balanced condition is easy to achieve. It is only necessary to meter the current in the variable constraint and adjust the voltage to minimize it. The fixed constraint current may then be measured and the input admittance at the fixed constraint determined.

With two or more variable constraints, the procedure is not so simple. Several methods of approach to the problem will be discussed.

The first method might be termed the "Matrix Method". If there are  $n-1$  variable constraints applied to the network, the input currents may be expressed as a linear combination of the constraining voltages:

$$\begin{array}{rcl}
 b_{11}V_1 + b_{12}V_2 + \dots & = & I_1 \\
 b_{21}V_1 + b_{22}V_2 + \dots & = & I_2 \quad (\text{III-6}) \\
 \vdots & & \vdots \\
 b_{n1}V_1 + b_{n2}V_2 + \dots & = & I_n
 \end{array}$$

The coefficients have the dimensions of admittance and are, in fact, the input and transfer admittances associated with the network. These values may be measured directly on the analog by setting each voltage in turn to a standard value while keeping the others zero and measuring

the resulting currents. Note that when the network is symmetrical only  $n(n+1)/2$  coefficients need be measured as against  $n^2$  in the unsymmetrical case. If desired, the coefficients could be calculated from the original network equations by taking ratios of determinants of the proper minors.

In order to make the variable constraint currents vanish, set  $I_2, I_3, \dots, I_n$  equal to zero and discard the first equation. The remaining equations are solved for  $V_2, V_3, \dots, V_n$  in terms of  $V_1$ , the fixed constraint. If these values are set on the analog, the resultant variable constraint currents should be zero, and the input admittance of the fixed constraint can be calculated from voltage and current measurements.

Of course, the last step is unnecessary, except as a check that the residual currents in the variable constraints are zero, for equations III-6 may be solved directly for the input admittance at point 1. Again taking all currents save  $I_1$  zero, solution for  $I_1$  by Cramer's rule (Ref. 10, pg 85) gives

$$Y_{11} = \frac{\Delta}{\Delta_{11}} \quad (\text{III-7})$$

where  $\Delta$  is the determinant of the coefficients and  $\Delta_{11}$  the determinant of the first order minor obtained by striking out the first row and column.

Often the labor of the previous method may be eliminated by a judicious choice of constrained points and by other techniques. Several examples will serve to illustrate this point.

First consider a one dimensional system typified by the circuit of figure 3. The first two modes are easily found, as previously indicated. The lowest mode has no nodes (see Section 2.3). Assume the node of the second mode is as indicated by  $N_2$ . The three constraints (presumed sufficient for obtaining the third mode) are taken at  $C_3$ . Note that free oscillation at second mode is suppressed by the constraints within the subregions separated by  $N_2$ . Now adjustment of  $C_{3a}$  will affect the currents in  $C_{3a}$  and  $C_{3b}$  only, due to the isolating effect of  $C_{3b}$ . Similarly, variation of the voltage at  $C_{3c}$  affects the currents at  $C_{3b}$  and  $C_{3c}$  only. By alternate adjustment of  $C_{3a}$  and  $C_{3c}$  it is possible to achieve current minimum in all the constraints quickly. This is essentially a process of reducing "residues" by a relaxation technique as illustrated numerically by several authors, notably Southwell (Ref. 18). The advantage here is that residues accrue at only three points rather than the seven of the basic circuit.

Another technique which may be used in a one dimensional circuit is suggested by the isolating properties of a single constraint. Since the current in  $C_{4a}$ , say, may be made zero simply by adjustment of the voltage at  $C_{4a}$ , without affecting either the voltage or current at  $C_{4c}$  or  $C_{4d}$ , it follows that this current may be maintained zero by keeping the ratio of voltages at  $C_{4a}$  and  $C_{4b}$  at the correct value. This might be done by use of an auxiliary transformer. The current in  $C_{4b}$  would next be made zero by adjustment of  $C_{4c}$  or of  $C_{4a}$  and  $C_{4b}$  simultaneously. In this manner the residue is "washed" off the right hand end of the circuit.

The circuit of Figure 4 is typical of the equation for beam bending (Ref. 3 and 19). Though this is still a one dimensional system, the

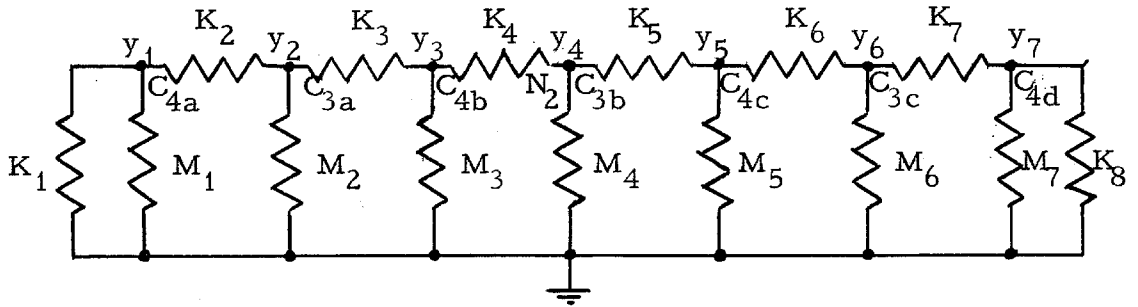


Figure 3. Placement of Constraints - Single Space Variable

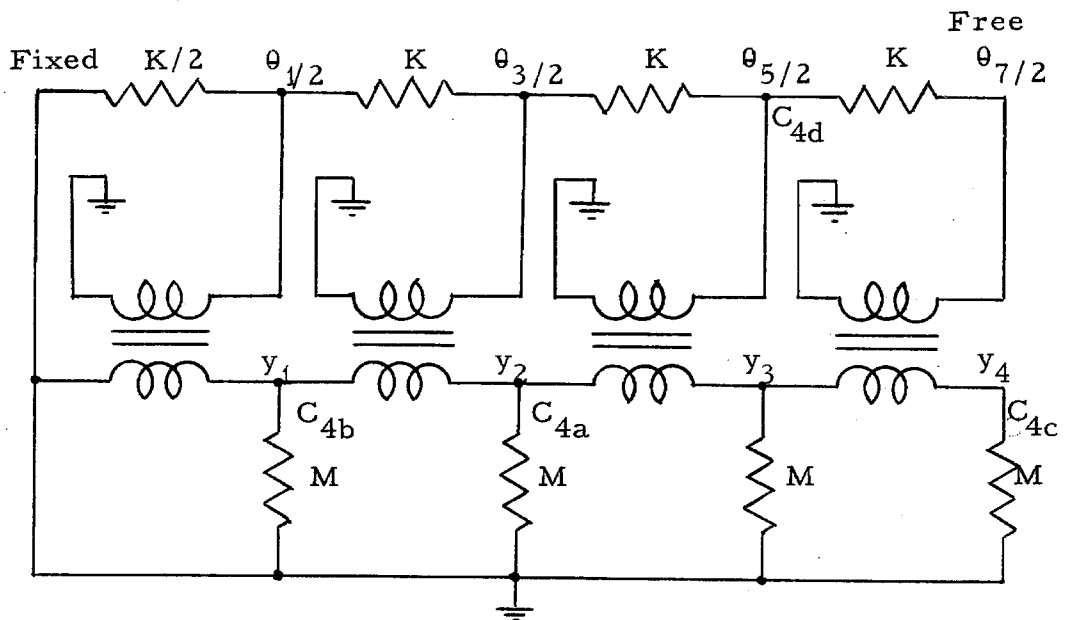


Figure 4. Placement of Constraints - Beam Analog



transformer coupling prevents a single constraint from isolating two other constraints. It is seen that both  $C_{4a}$  and  $C_{4d}$  are required to prevent  $C_{4b}$  from affecting  $C_{4c}$ .

If a metering circuit is devised to form the sum of the magnitudes (or squares of the magnitudes) of the constraint currents, the voltages may be adjusted in a correct manner by always causing this quantity to decrease. (Ref. 20, pg. 13, Ref. 21).

Another method has been tried which depends on the fact that the total power driving the network has a stationary value when all the currents except that in the fixed constraint are zero. The total power may be expressed as a quadratic form by multiplying the first of equations III-6 by  $V_1$ , the second by  $V_2$ , etc., and summing:

$$P_{in} = \sum_i \sum_j b_{ij} V_i V_j. \quad (\text{III-8})$$

A stationary value is found by solving the  $n-1$  equations (remembering that  $V_1$  is fixed)

$$\frac{\partial P_{in}}{\partial V_j} = 2 \sum_i b_{ij} V_i = 0; \quad (j = 2, 3, \dots, n) \quad (\text{III-9})$$

Except for the factor of 2, these are exactly the equations obtained in the previous method when solving for the voltages required to make all the variable constraint currents zero. The condition of stationary power input is, then, the condition which it is desirable to achieve.

This stationary value is

$$P_{st} = V_1^2 \frac{\Delta}{\Delta_{11}}, \quad (\text{III-10})$$

In this equation, as is also the case in (III-7), the  $\Delta$ 's may refer either to the matrix of coefficients of (III-6) or to the admittance coefficients of the original system equations, whichever viewpoint is more convenient for the purpose at hand.

Expanding the power input in a Taylor series about the stationary point (Ref. 23, Vol. II, pg 78) gives

$$P_{in} = P_{st} + \sum_{i=2}^n \sum_{j=2}^n b_{ij} V_i V_j \quad (\text{III-11})$$

The type of stationary point is determined by the matrix of the coefficients  $b_{ij}$ . If the matrix is positive definite, the point is a minimum; if negative definite, it is a maximum. If it is neither, the point is a saddle point in the multidimensional space of the problem. A simple example (Section 5.2) shows that one cannot always assure definiteness in these problems.

In summary, it has been shown that the inherent instability of the analogy may be controlled by the use of constraints on some of the coordinates. Use of the constraints changes the system equations and one of several methods must be used to eliminate extraneous currents (forces).

## IV. CONSTRUCTION OF THE COMPUTER

The discussion of Part III has indicated a major construction problem: the synthesis of a suitable negative conductance element. The actual circuits used by the author will be presented here, with a discussion of the properties required in addition to those specified in Part III. The author has become well aware of some of the drawbacks and deficiencies of these circuits in the course of time and has included some remarks on possible improvements in the conclusions - Part VI.

#### 4.1 Primary Considerations

The most obvious requirements on negative conductance generators are implicit in the discussions of Parts II and III. They are:

- i) All negative conductances should be capable of independent setting of the basic value of conductance.
- ii) Once set for a particular problem, a single continuously variable control adjusts the value of all conductances simultaneously maintaining the ratio of one to the other as determined by the basic values. This control is termed the eigenvalue control or, more loosely, the frequency control.
- iii) If transformers are to be used, a basic frequency must be established. No direct current may flow in the output of the generators in order to prevent saturation of transformer cores.
- iv) As a matter of convenience, adjustments to the generators should be simple and unaffected by changes in value of negative conductance. represented, within a reasonably large range. The power handling capabilities of the generator should be adequate for all contemplated resistance levels.
- v) It may be necessary to consider cost and space limitations.

#### 4.2 Negative Conductance Generators

If a positive conductance is connected across a voltage source, the current which flows through it is proportional to the voltage and the conductance, in accordance with Ohm's Law. The direction of current flow is as indicated in Figure 5a. If the conductance is negative, the current flow is reversed as in figure 5b. That such an element cannot be synthesized from passive elements is obvious, as in energy considerations (Ref. 17, pg. 126), for example.

A circuit for a generator operating in a direct current computer has been used by Swenson, (Ref. 7, 8, 9) figure 6 (with  $\alpha = 1/2$ ). In operation, the circuit is adjusted until the voltmeter indicates zero. At this point  $e_d = v_n$  and the input admittance is

$$Y_i = -G_n \quad (\text{IV-1})$$

The circuit may, of course, be used with fixed frequency alternating current by replacing the battery with an a. c. source.

If the value of  $\alpha$  is not taken equal to  $1/2$  but is allowed to vary, the input admittance in the balanced condition is given by

$$Y_i = -G_n \left( \frac{1 - \alpha}{\alpha} \right) \quad (\text{IV-2})$$

Since  $0 \leq \alpha \leq 1$ ,  $1 \leq \frac{1}{\alpha} \leq \infty$  so that all values of negative admittance may be covered with this generator.

The second requirement of Section 4.1 is that all the negative conductances in an analog should be capable of being adjusted simultaneously to be proportional to the eigenvalue setting. The generator of figure 6 may be used in this manner by ganging the potentiometers to the same shaft. It is apparent that the admittances of generators so connected will be proportional to their respective  $G_n$  settings. The difficulty

with this type of generator is that each generator requires hand balancing for each setting of the potentiometers. In fact, it is easily seen that one adjustment will not usually be sufficient as each generator's terminal voltage will depend on that of all the others.

One solution is immediately obvious: provide servo balancing of the generators. This requires some sort of differential amplifier connected to the terminals previously used for the voltmeter, as in figure 7, but is otherwise straightforward.

By using positive-gain amplifiers, it is possible to eliminate the servo motors as in figure 8. The input admittance of this circuit is

$$Y_i = -G_n (A \alpha - 1) \quad . \quad (IV-3)$$

the input admittance of the potentiometer being excluded. This circuit has the advantage that the admittance is directly proportional to the potentiometer setting, so that a linear scale may be used. The low output impedance (at  $e_1$ ) of the servo balanced model of figure 7 is much more difficult to achieve here.

The generator used in the computer constructed by the author is based on the final configuration above. The deciding factors were chiefly considerations of linear control scale, cost, compactness and ease of adjustment, since all of these models may be made to satisfy the first three requirements of 4.1.

Figure 9 presents a block diagram of the generator used in the computer. It consists basically of two high gain amplifiers with resistor feedback. Each amplifier has  $180^\circ$  phase shift so that the net phase shift is zero. The eigenvalue control potentiometer is placed after the first amplifier to avoid loading of the computing circuits. The role of the RC network between the amplifiers will be discussed in section 4.7.



Figure 5. Direction of Current Flow in Positive and Negative Conductances

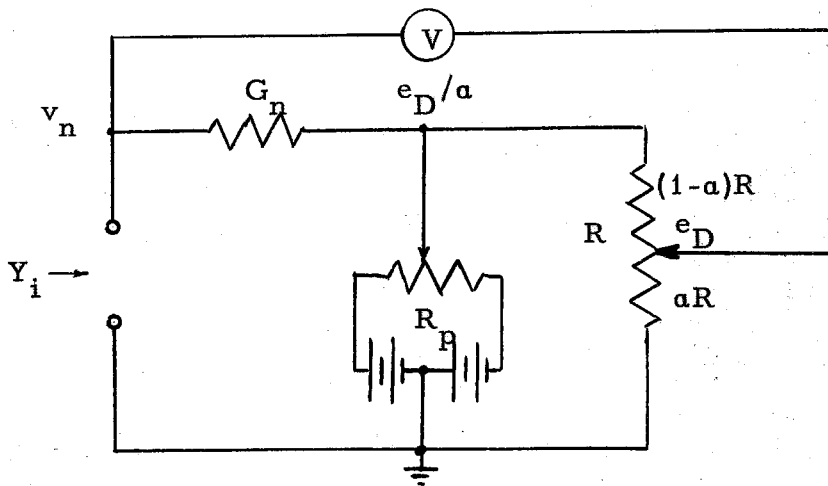


Figure 6. Direct Current Negative Conductance Generator

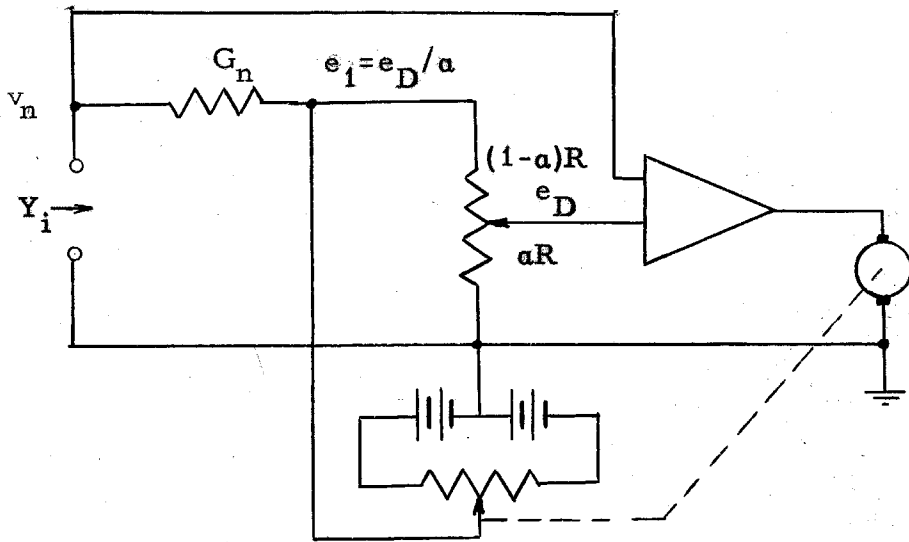


Figure 7. Servo Operated Negative Conductance Generator

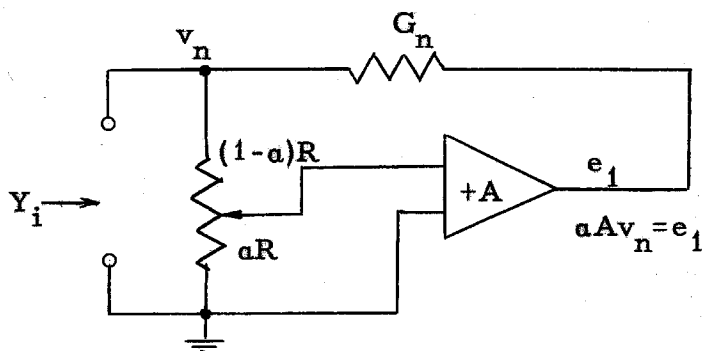


Figure 8. Electronic Negative Conductance Generator

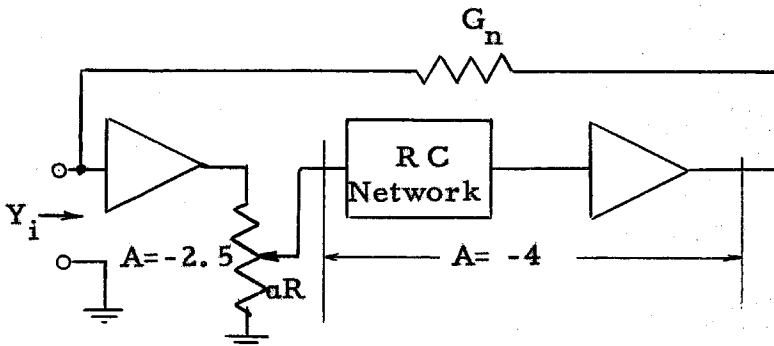


Figure 9. Block Diagram of Negative Conductance Generator

The overall gain of the two amplifiers and network is adjusted to be 10. This allows  $\lambda$  to vary from 0 to 9 as the potentiometer is varied from 1/10 full scale to full scale. The potentiometers used are ten turn Helipots, 10000 ohms and .5% linearity. When properly aligned, the 10 turn vernier dial is set so that the eigenvalue can be read directly.

#### 4.3 R-C Coupled Feedback Amplifiers

In an effort to minimize power supply requirements and the drift and oscillation troubles common to d.c. amplifiers, it was decided to construct the amplifiers with R C interstage coupling. However, since the working frequency was selected to be 150 cps, it was not without some difficulty that a stable feedback amplifier was constructed. The choice of frequency is based on the desirable operating range of the California Institute of Technology Analysis Laboratory transformers to be used in the analogs, and on a desire to keep away from the higher harmonics of the 60 cycle line current. The circuit schematic for the input amplifier is drawn in figure 10.

When a three stage R C coupled amplifier is to be used as a feedback stabilized computing amplifier, there is a definite limit to the allowable loop gain, due to the accumulated phase shift at frequencies far from the center frequency. The loop gain limit may be varied somewhat by judicious choice of the R C products.

Treating the amplifier as equivalent to three high-pass R-C L-sections isolated by buffer amplifiers leads to the following results:

- 1) Maximum gain at  $180^\circ$  phase shift occurs when one time constant is equal to the geometric mean of the others. Minimum gain occurs when two time constants are equal.



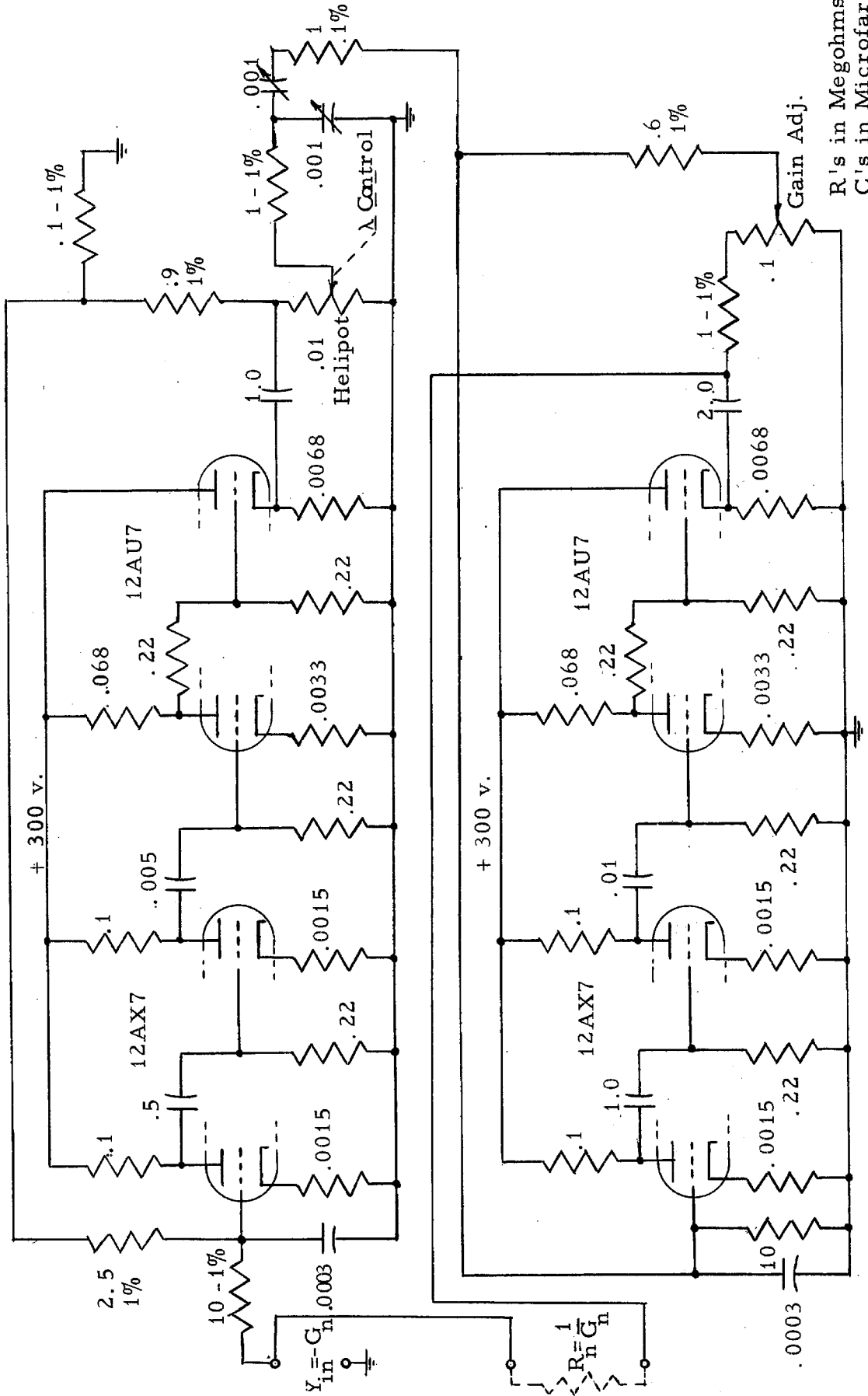


Figure 10. Negative Conductance Generator - Schematic

ii) If  $R^2$  is the ratio of the largest time constant to the smallest, the maximum gain is

$$K_{\max} = \frac{R^2}{(1 + R^2)(1 + R)^2} \quad (IV-4)$$

The minimum gain is given by

$$K_{\min} = \frac{R^2}{2(1 + R^2)^2} \quad (IV-5)$$

These are plotted in figure 11.

If there is no phase shift introduced by the feedback, the allowable loop gain at mid-frequency is  $1/K$ , with no gain margin allowance.

As an example take an amplifier with the following constants:

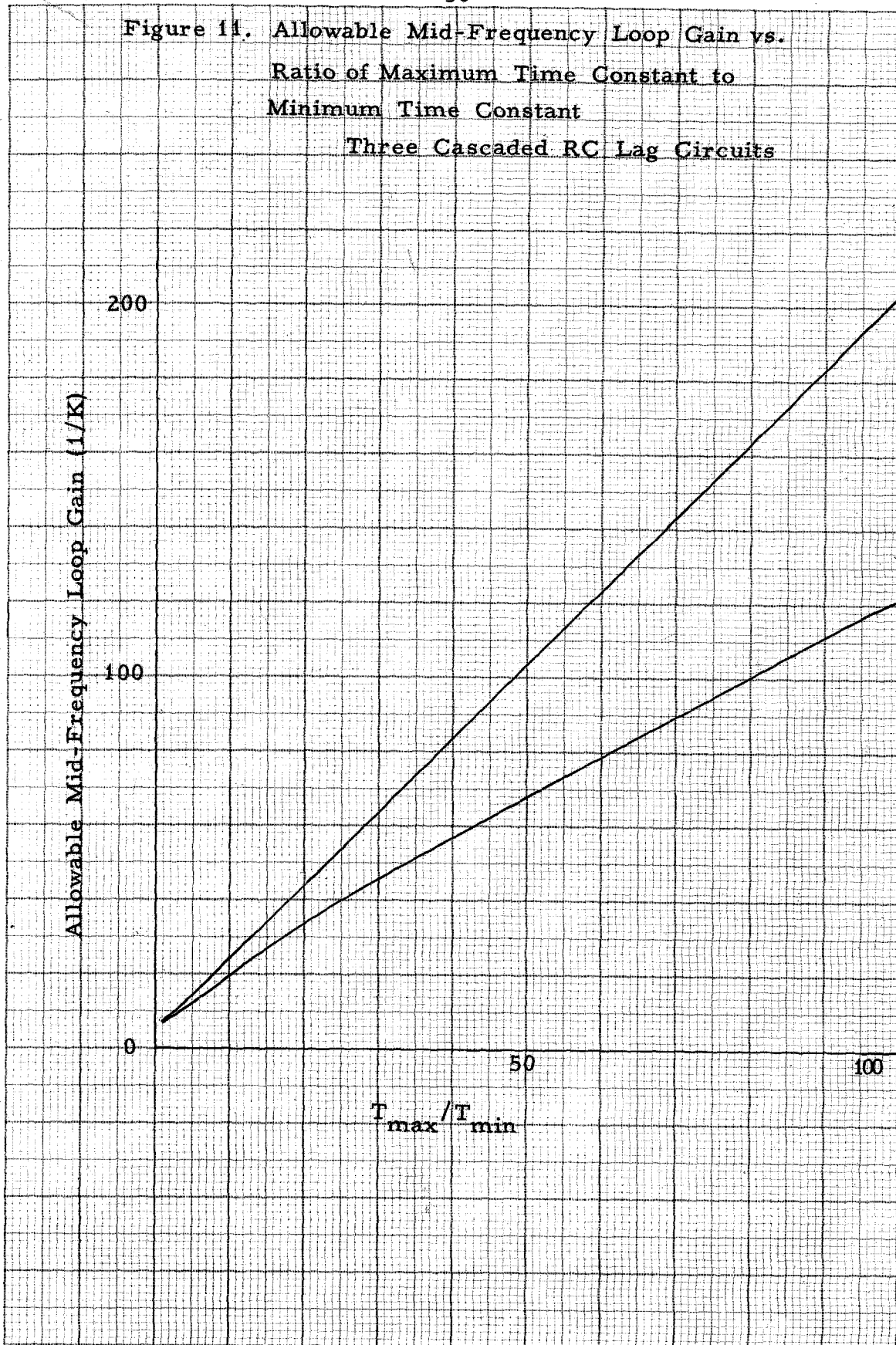
$$\begin{aligned} T_1 &= .0014 & R &= 10 \\ T_2 &= .14 & A_m &= 1350 \end{aligned}$$

If  $T_3$  is allowed to vary and if for some methods of operation it may take on the value  $R$ , the amplifier must be designed to be stable with  $K = K_{\max} = .0082$ . Then the gain at  $180^\circ$  phase shift is  $K_{\max} A_m = 14.3$ . This is the factor by which the loop gain must be reduced at  $\omega_{K_{\max}}$ .

If the feedback is constant with frequency the maximum loop gain at  $\omega_0$  is  $1/K_{\max} = 122$ . Reduction to 40-50 allows adequate gain margin. The input amplifier of the generator, figure 10, has the constants above with  $T_3 = .0.1$ . The feedback illustrated gives a measured loop gain of 42 at 150 cps.

The output amplifier is more of a problem as the output time constant depends on the value of  $G_n$  used in the circuit. Furthermore, there is additional phase shift produced by the loading of the network between the amplifiers. It was found necessary to reduce the loop gain of this amplifier to about 10 for stability reasons when the load resistance  $R_n = \frac{1}{G_n}$  was set at 500 ohms in some circuits.

Figure 11. Allowable Mid-Frequency Loop Gain vs.  
Ratio of Maximum Time Constant to  
Minimum Time Constant  
Three Cascaded RC Lag Circuits



Tendency to oscillate at high frequencies was stopped by employment of small condensers from input grid to ground as shown in the circuit diagrams. This method with its high frequency gain reduction is allowable here because of the single frequency of interest.

#### 4.4 D. C. Amplifiers

In effort to increase the loop gain and thus lower the output impedance of the final amplifier, a direct coupled amplifier requiring an additional -150 volt power supply was constructed, Figure 12. The loop gain of this amplifier is 40 at the working frequency and it is stable for the high values of  $G_n$  required. There is no low frequency oscillation trouble as in the a-c amplifier, for there is but one R-C lag in the circuit and the maximum phase shift is  $90^\circ$ .

#### 4.5 Dual Locus Nyquist Diagrams

In anticipation of the discussion of the following section, the dual locus Nyquist diagram, an extension of the conventional Nyquist diagram, will be presented. This section is essentially a review of pertinent parts of reference 24, which should be consulted for more detailed diagrams and examples.

Consider a dynamical system with characteristic equation  $F(p) = 0$ , where  $F(p)$  is a polynomial in  $p$ , the complex frequency variable. In many of the cases encountered servo mechanism and feedback amplifier analysis, this equation appears in the form

$$1 + G(p) = 0. \quad (\text{IV-6})$$

where  $G(p)$  is a quotient of polynomials in  $p$ . The Nyquist criterion

(Ref. 17) for stability consists in making a polar plot of  $1 + G(j\omega)$  as  $\omega$  varies from 0 to  $\infty$ . If the plot encircles the origin, the system is unstable. Systems with zeros in the right half plane are not considered.

In some cases it is simpler to consider the characteristic equation to be of the form

$$F(p) = A(p) + B(p) = 0 \quad (\text{IV-7})$$

If the functions  $-A(j\omega)$  and  $+B(j\omega)$  are plotted, along with  $F(j\omega)$ , figure 13, it is seen that the magnitude and direction of  $F$  at any frequency may be obtained from plots of  $-A$  and  $+B$  by use of the equation

$$-A(j\omega) + F(j\omega) = B(j\omega). \quad (\text{IV-8})$$

A little consideration shows that it is not necessary to plot  $F$ , for it is sufficient to visualize the direction of the vector  $F$  as  $\omega$  increases from 0 to  $\infty$  in order to see if it encircles the origin. With this in mind it is easy to see that the system must be stable if the two loci do not intersect--unless one lies wholly within the other in which case the system must be unstable.

If the two loci intersect the situation must be examined more closely. In order for the system to remain stable the locus first reaching the intersection, (that is, reaching it at a lower value of angular frequency) must also be the first to reach the second intersection (figure 14). It will be noted that it has been unnecessary to point out which locus is that of  $A(j\omega)$  and which that of  $-B(j\omega)$ .

If the  $\omega = \infty$  point of one locus lies within a region surrounded by the second, then the second must reach the point of intersection at the lower frequency. If the  $\omega = 0$  point is within such a region, then this locus must reach the point of intersection first. Loci which become infinite as  $\omega \rightarrow \infty$  must have the closure at infinity taken into

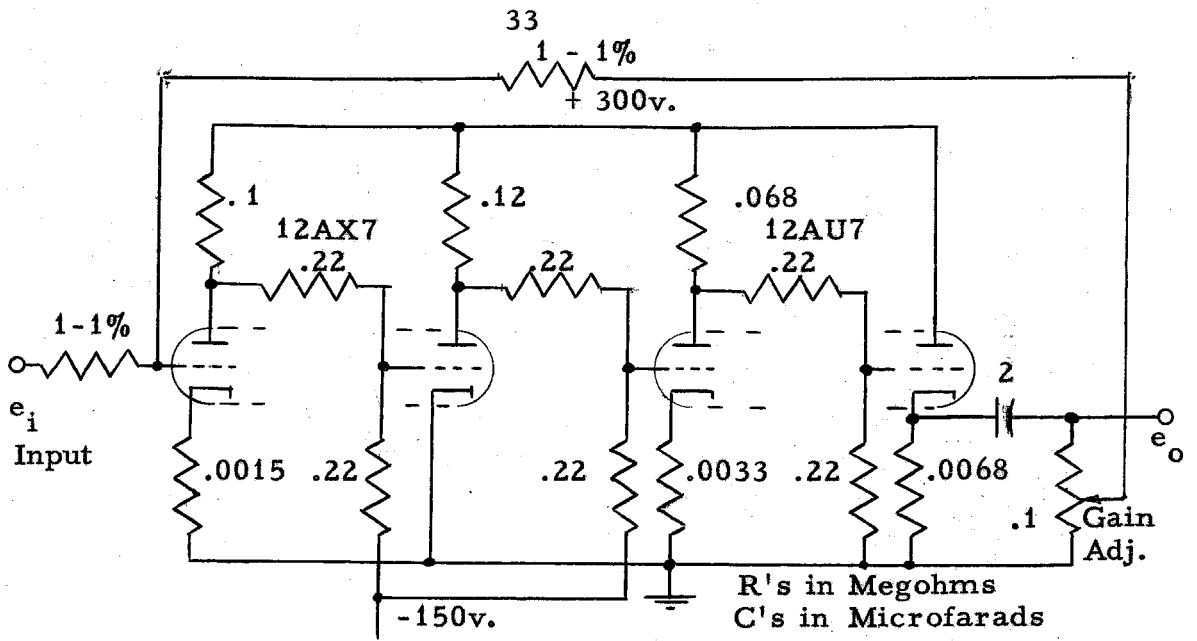


Figure 12. Direct Coupled Amplifier

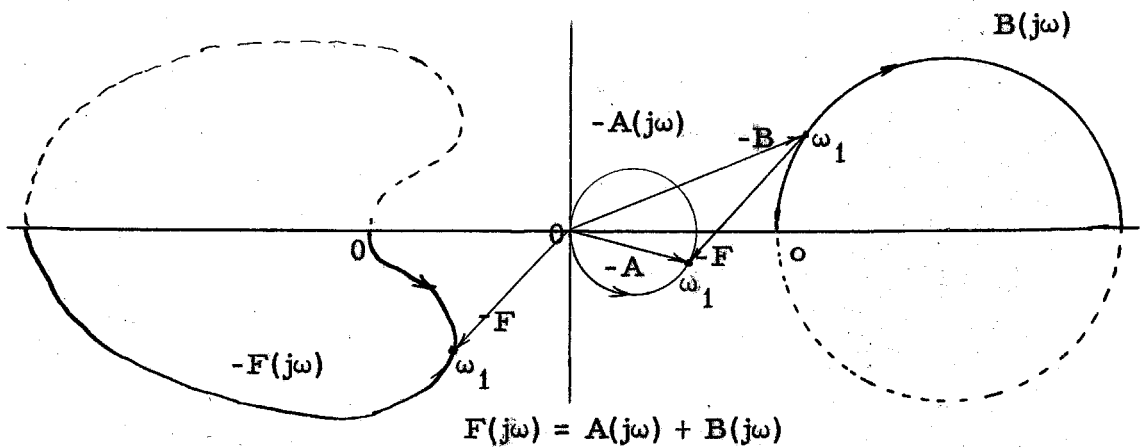


Figure 13. Construction of the Sum of Two Loci

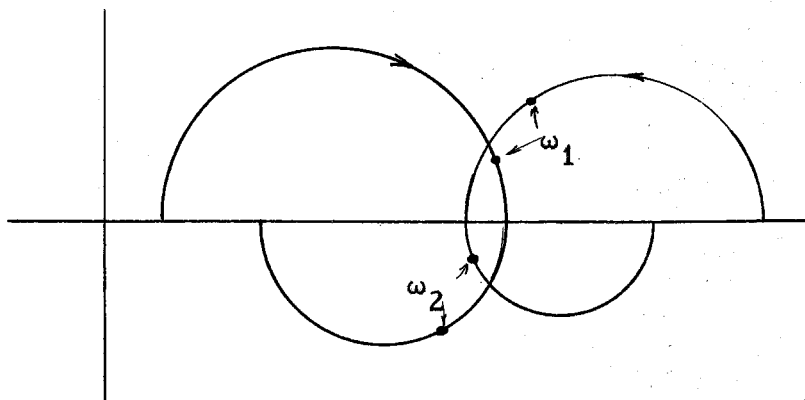


Figure 14. Dual Locus Nyquist Diagram - Illustrating Stability

account in order to apply these criteria.

#### 4.6 Effect of Parasitic Impedances

It has been shown in Part III that an analog including many active impedances can be constrained so as to prevent oscillations which would make it impossible to obtain the second and higher eigenvalue and eigenvectors. The discussion there was based on the assumption that all networks were purely conductive and that all negative conductance generators were identical. Construction of such networks is impossible, of course, due to the inevitable wiring reactance, the magnetizing and leakage inductance in transformers and uncompensated phase shift in the amplifiers.

The problem facing the designer is this: What should the frequency response characteristics of the generator be in order to maintain accuracy and avoid spurious oscillations for all types of parasitic effects which may reasonably be expected? The problem will be approached by analyzing, qualitatively, several typical examples. Dual locus Nyquist diagrams will be used (See Section 4.5). Since the characteristic equation of the interconnected system can be factored as shown in Section 3.3, the circuit of figure 15 will serve for all cases. Here a single generator is isolated and the remaining portions of the circuit are lumped in the effective admittance  $Y_e$ . Effects of parasitics in the circuit or within the isolated generator are accounted for by taking  $Y_g$  and  $Y_e$  to be other than pure conductances.

The characteristic equation of the circuit is

$$Y_e - Y_g \{A(p) \alpha - 1\} = 0, \text{ or} \quad (\text{IV-14})$$

$$\left( \frac{Y_e}{Y_g} + 1 \right) - \alpha A(p) = 0 \quad (\text{IV-15})$$

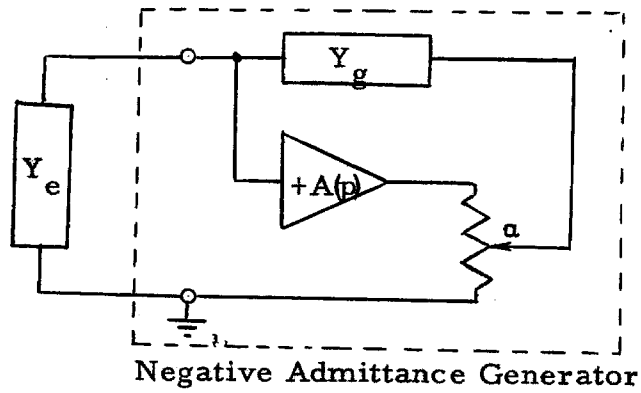


Figure 15. Model for Parasitic Study

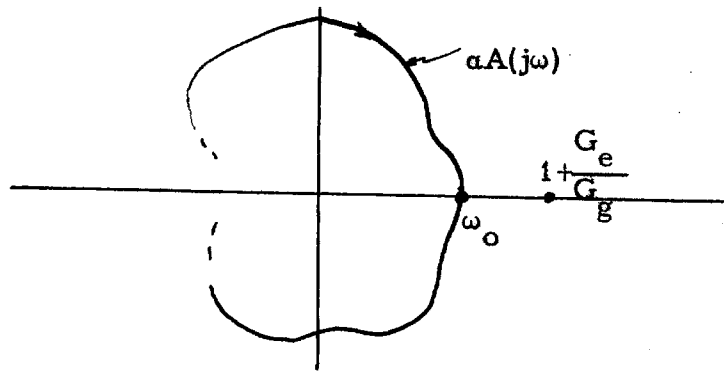


Figure 16. Dual Locus Nyquist Diagram - Case I Pure Conductance

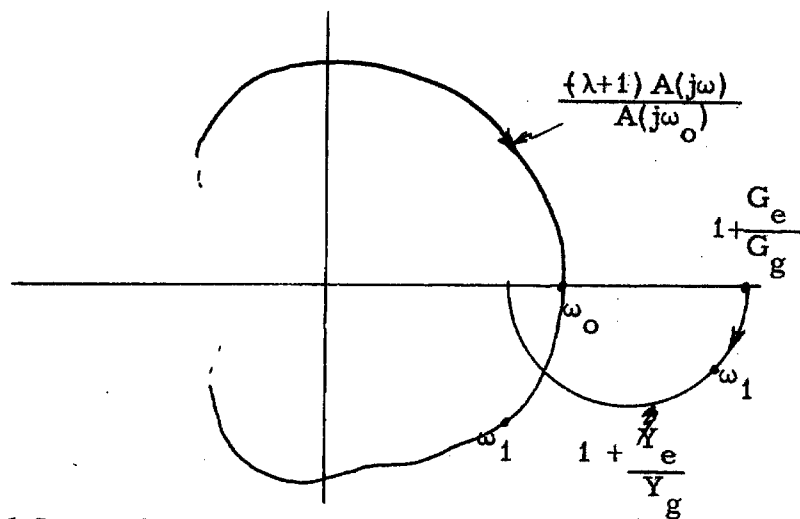


Figure 17. Dual Locus Nyquist Diagram - Case II Series Inductance



## Case I

The ideal or purely conductive case discussed in Part III (especially 3.3) occurs for  $Y_g = G_{gn}$  and  $Y_e = G_e$ . This case is illustrated in figure 16. The circuit will oscillate when, by variation of  $\alpha$ , the locus of  $\alpha A(j\omega)$  passes through  $1 + G_e/G_n = B(j\omega)$ . Noting this and (III-2), we see that the circuit is properly adjusted when

$$\alpha = \frac{\lambda + 1}{A(j\omega_0)} \quad . \quad (IV-16)$$

This means, since  $\alpha$  and  $\lambda$  are real, that the amplifier must have no phase shift at the working frequency.

## Case II

$$Y_e = \frac{1}{R_e + Lp} \quad , \quad Y_g = G_g$$

This case illustrates the possible effect of the distributed inductance if wire-wound resistors are used in the computer. In this

$$\text{case } \frac{Y_e}{Y_g} = \frac{1}{G_g(R_e + Lp)} = \frac{G_e}{G_g} \frac{1}{1 + L G_e p}$$

The locus is a semicircle lying below the real axis, figure 17. Oscillations occur when the frequencies of the two loci are the same at their point of intersection. It is desirable, of course, to have this instability occur with the  $\omega_0$  point of  $\alpha A$  as close as possible to the zero frequency point of  $1 + Y_e/Y_g$ . This becomes more nearly the case as the change of phase shift with frequency is decreased for  $1 + Y_e/Y_g$  (smaller parasitic inductance) or increased for  $\alpha A$ . It may be noted that if the circuit conductances all have the same percentage parasitic

inductance we have  $\frac{Y_e}{Y_g} = \frac{G_e(1 + G_g L_g p)}{G_g(1 + G_e L_e p)} = \frac{G_e}{G_g}$ , and the problem reduces to

Case I.

Case III

$$Y_e = G_e + Cp \text{ or } Y_e = G_e + \frac{1}{L p}. \quad Y_g = G_g$$

Other parasitic reactances may appear as either capacitance or inductance in parallel with the resistances. Both these loci are covered by the straight line in figure 18. There is no trouble with accuracy in this case so long as the magnitude of  $A(j\omega)$  is greatest at  $\omega = \omega_0$ . Thus, loci such as are shown dotted in the figure are not to be allowed.

Case IV

$$Y_e = \frac{G_e}{1 + LG_e p} + Cp, \quad Y_g = G_g.$$

There is usually a capacitance shunting the external impedance due to wiring, etc., which may be of a magnitude to cause trouble at frequencies far from  $\omega_0$ . This case illustrates the possibility of high frequency instability if  $LG_e > \frac{C}{G_e}$ . This is the condition illustrated in figure 19. It occurs when the gain of the amplifier is allowed to increase at high frequencies, as may occur, for example, by capacitive pickup from adjacent leads.

#### 4.7 Generator Frequency Response Requirements

The requirements placed upon the frequency response of the negative conductance generator by the analysis of the previous sections are:

- i) Positive gain, no phase shift at a specified working frequency,  $\omega_0$ .
- ii) A high value of frequency gradient at  $\omega_0$ .

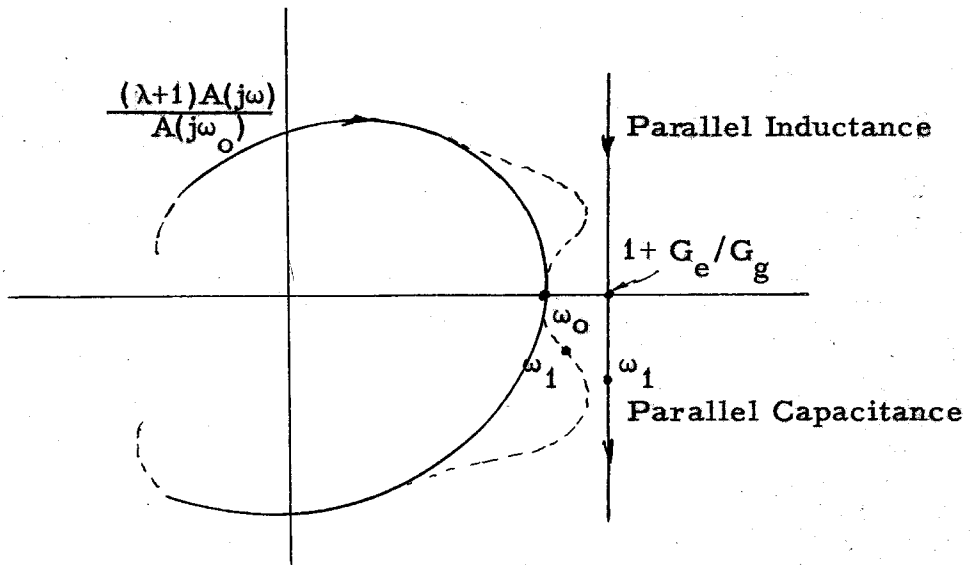


Figure 18. Dual Locus Nyquist Diagram - Case III Parallel Reactance

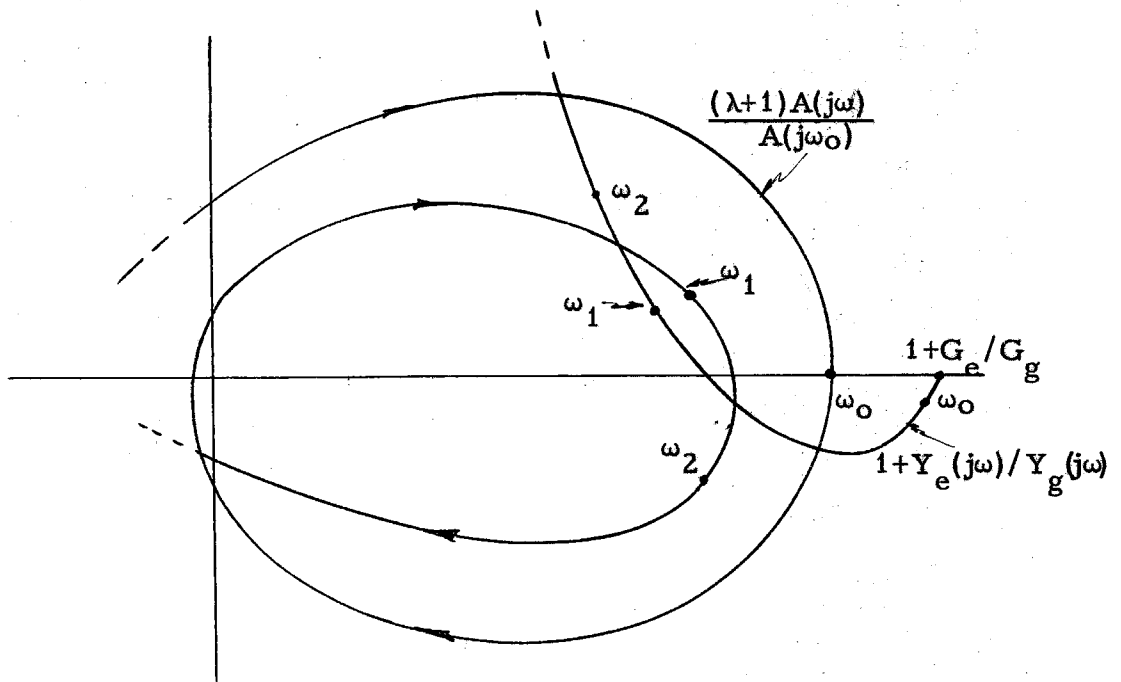


Figure 19. Dual Locus Nyquist Diagram - Case IV Illustrating High Frequency Instability

iii) Rapid decrease in gain for frequencies far from  $\omega_0$ .

These, together with the requirements of 4.1, specify the type of generators to be built.

The above three requirements are met by introducing the shaping network of figure 20 between the two stabilized amplifiers figure 9: The locus of the transfer function of this network is a circle in the complex frequency plane, and, of course, the values are chosen to make the phase shift zero at  $\omega_0$  - 150 cycles per second for this computer. The capacitances are made variable to allow for compensation of the inevitable small phase shifts occurring in the amplifiers.

The generators are adjusted by setting the  $\lambda$  control to 1.0 and adjusting the trimmers of the shaping network and the fine gain adjustment to give zero phase shift and a gain of 2 at  $\omega_0$ . This is most easily accomplished by "resonating" a selected  $G_g$  with an equal value of  $G_e$  as in figure 21. Satisfactory current minima of 8-15 microamperes were obtained on the generators of the computer.

#### 4.8 Test Results

The block diagram of the negative conductance generator used in the computer is shown in figure 9. The network between the amplifiers is described in section 4.7 and figure 20, and the amplifier schematic in figure 10. Several tests were made on typical amplifiers to see how well they could be expected to perform in analog circuits and to verify certain theoretical predictions.

The transfer function of the R-C filter is a circle in the complex plane. If the amplifier gain were constant at all frequencies the admittance of a typical generator would be as indicated in figure 22.

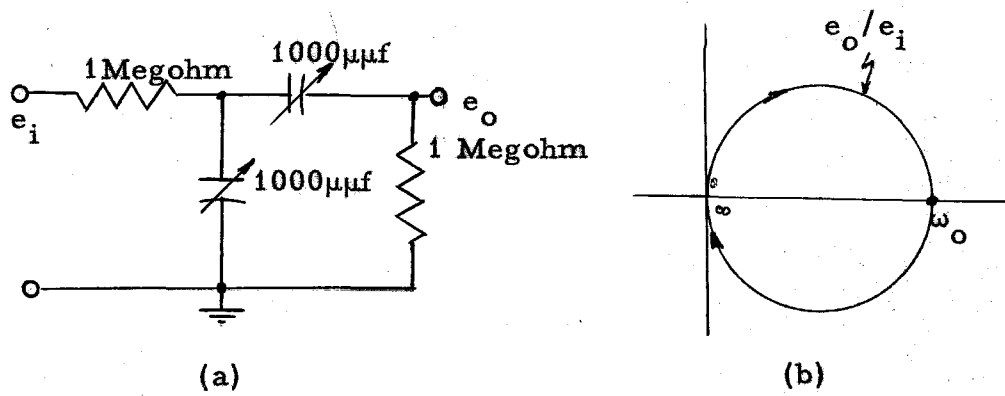


Figure 20. Shaping Network

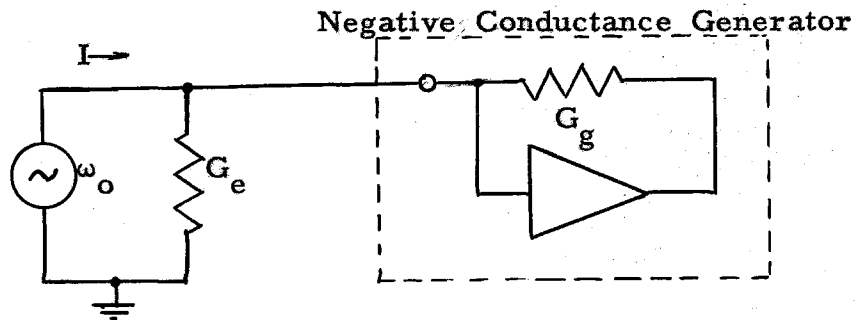


Figure 21. Circuit for Balancing Generator

○ — Ideal Transfer Function  
 × — Typical Generator

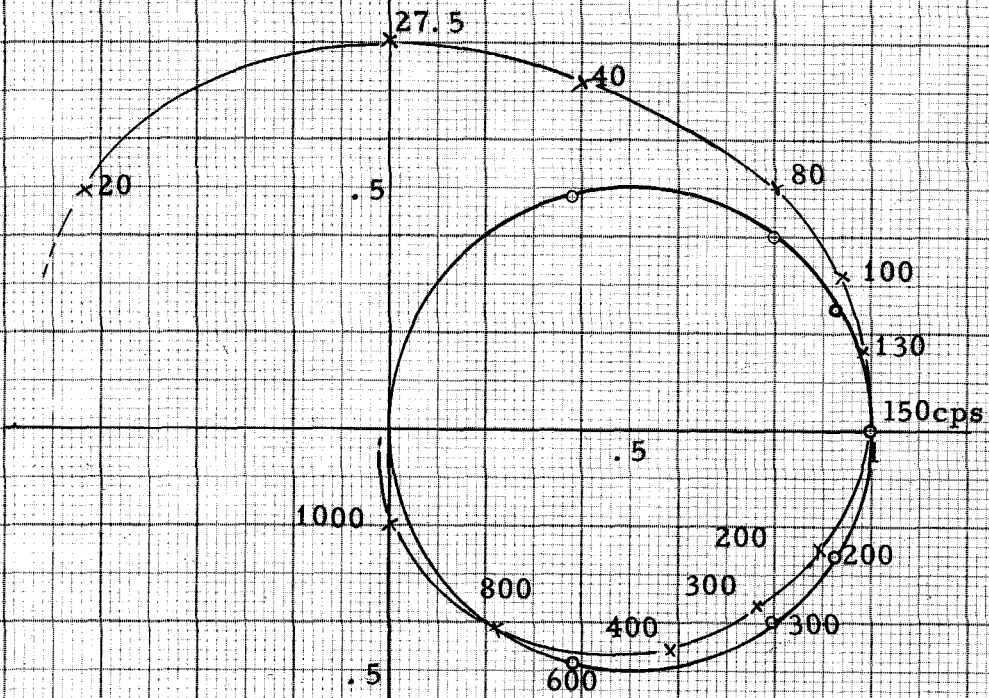


Figure 22. Frequency Response of Ideal Shaping Network and of a Typical Generator

The measured input admittance of a typical generator is drawn on the same sheet for comparison. Deviations are mainly due to the non-ideally-flat gain characteristics of the amplifiers.

Tracking of the input conductance with the  $\lambda$  control is, of course, necessary for successful operation. Table IV-1 and Figure 23 summarize the results of tests made on all of the generators. The circuit of Figure 21 was used to make the calibration with  $G_g$  fixed at  $10^{-3}$  mho and  $G_e$  variable. It is seen that the tracking is quite good over most of the range. The deviations near the middle of the range are due mainly to loading of the potentiometers by the R-C filter (Figure 9). Two methods might be employed to overcome this difficulty:

- i) Use the data of Table IV-1 to derive a calibration curve for correction of dial readings.
- ii) Use a resistor in series with the potentiometer to cause the variation to be over a more linear portion of the loading curve.\* This would also require higher gain in the initial amplifier to allow use of the same dial fixtures.

A further difficulty was encountered in the use of electronic amplifiers to generate negative conductance. This was associated with limitations on the current handling capacity of the output tube of the amplifiers. It was found that 31.5 volts rms was the maximum capacity of this particular circuit. Accordingly it became necessary to specify the maximum input voltage (terminal voltage of the negative conductance)

---

\* This and other methods of avoiding loading difficulties are discussed in Ref. 23, pg 95.

Table IV-1

## POTENTIOMETER ALIGNMENT

$$\text{Percent error} = 100. \frac{(\text{Measured voltage ratio}) - (\text{Dial setting})}{(\text{Dial setting})}$$

Dial  
Setting

	Percent Error						mean	rms
	1	2	3	4	5	6		
.10	.00	.00	-.40	.05	-.25	-.15	-.125	.203
.20	.00	-.25	-.15	.24	-.33	.06	-.07	.206
.30	.00	-.43	-.26	.24	-.41	.03	-.14	.28
.40	.05	-.24	-.25	.25	.50	.15	.08	.277
.50	-.15	-.58	-.57	-.12	.43	-.33	-.22	.406
.60	.13	-.06	-.16	.25	.75	.03	.155	.335
.70	.11	-.03	-.10	.20	.52	.03	.12	.236
.80	-.02	-.24	-.19	.05	.23	-.09	-.04	.162
.90	-.05	-.11	-.26	.00	.07	-.10	-.075	.127
1.00	-.15	-.24	-.28	-.07	-.11	-.26	-.19	.246



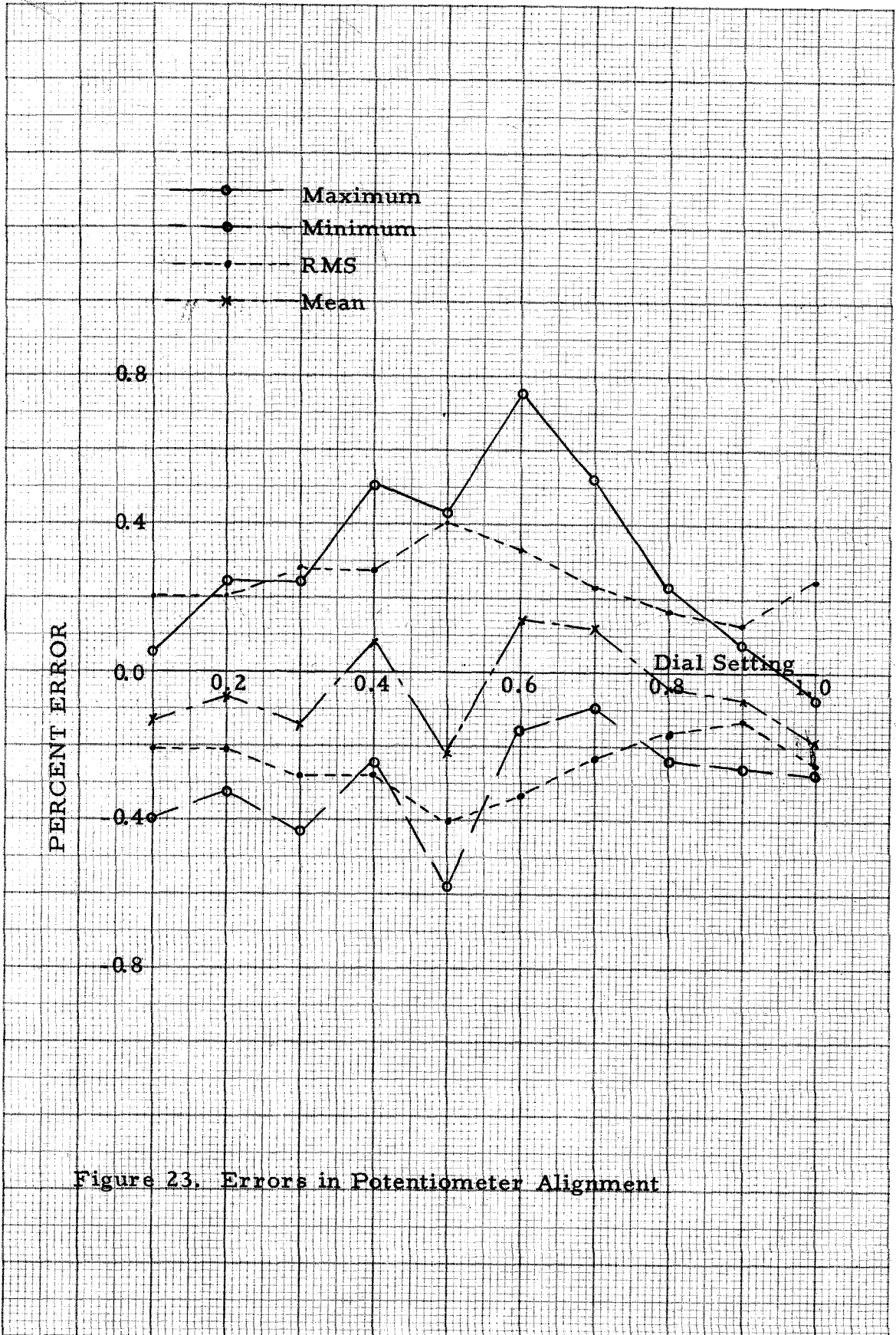


Figure 23. Errors in Potentiometer Alignment

allowable. This is a function of the value of  $G_g$ . Curves of the maximum allowable input voltage as a function of  $\lambda$  and  $R_g = 1/G_g$  are given in Figure 24.

Several tests to confirm the theory of section 4.6 were made. A typical case is illustrated in Figure 25 and all results are tabulated in Table IV-2. It is seen that the results give reasonable confirmation of the theory.

Table IV-2  
EFFECTS OF PARASITICS

Type of Parasitic*	Instability occurs at:	
	$\lambda$	frequency (c.p.s.)
None	1.00	150
Series L = .01 hy	1.00	152
= .05 hy	.995	155
= .1 hy	.995	160
= .25 hy	.96	182
= .5 hy	.82	207
Parallel C = .004 $\mu$ f	1.00	150
.01 $\mu$ f	1.00	148
.1 $\mu$ f	1.00	141

It is also of interest to determine how sensitive a generator is to setting of the  $\lambda$  dial. This sensitivity is indicated by the "resonance" curve of figure 26 which was measured on a particular

\* All tests are with  $G_g = G_e = .001$  mho.

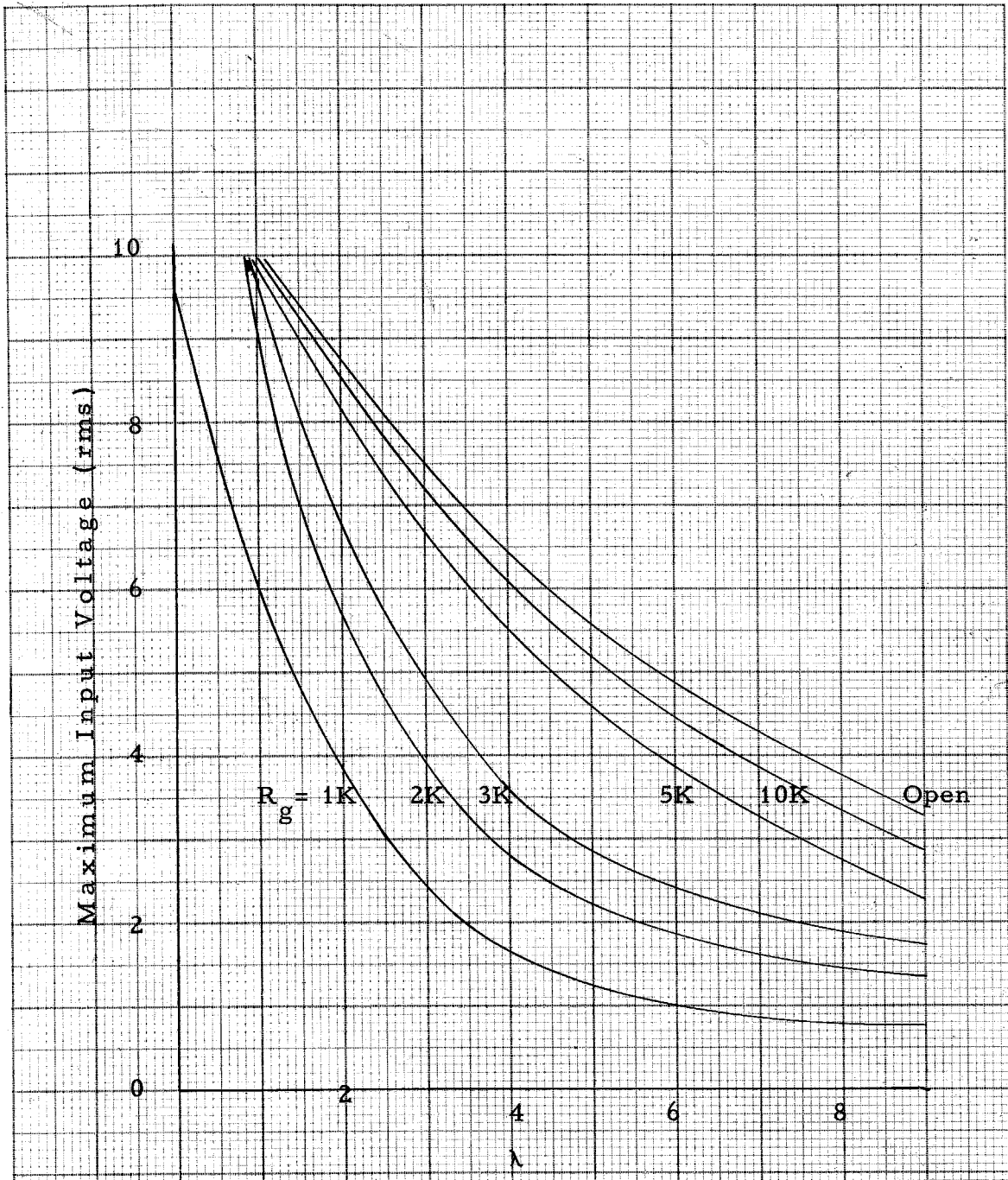


Figure 24. Maximum Allowable Input Voltage as a Function of  $\lambda$

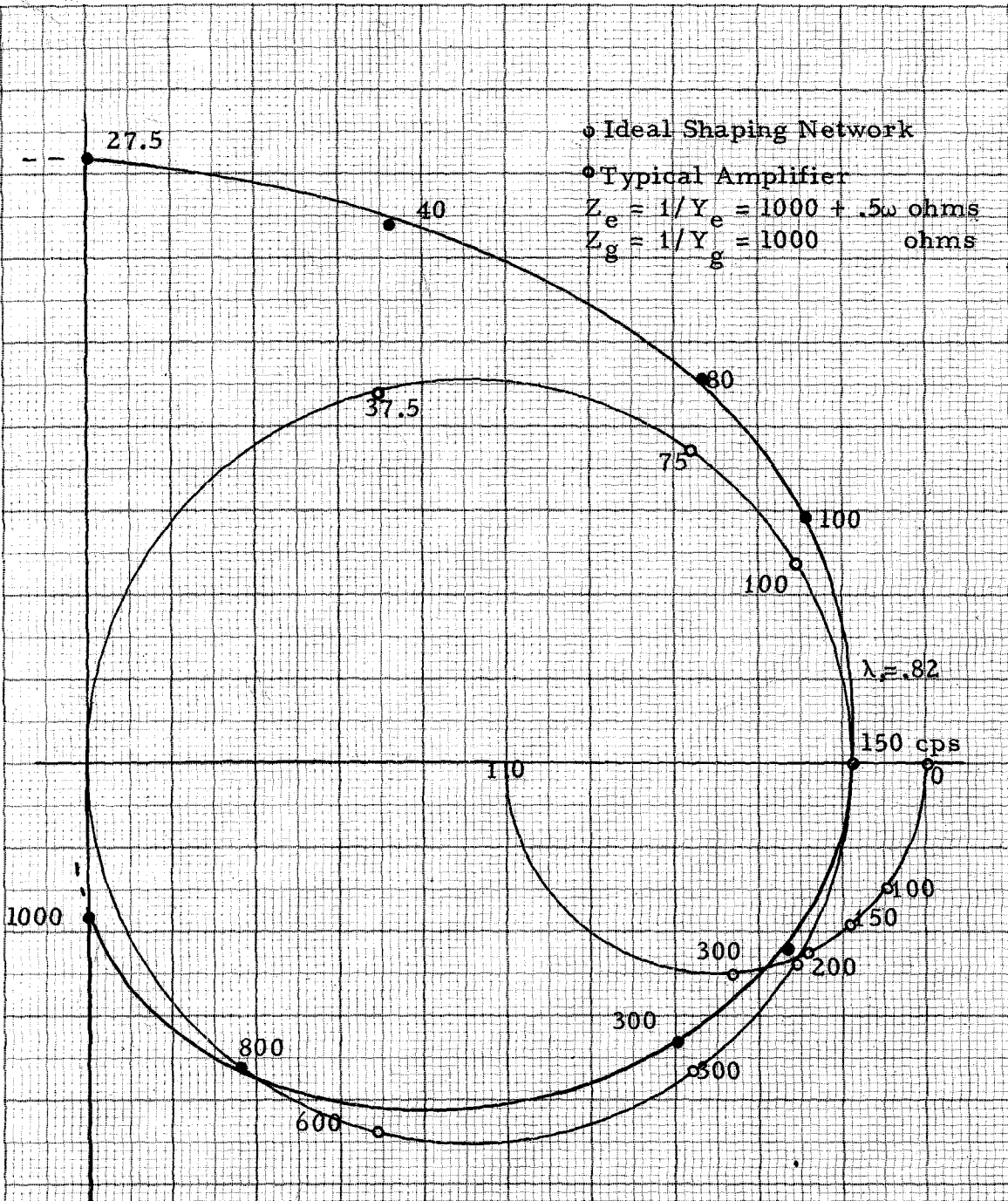


Figure 25. Dual Locus Nyquist Diagram Showing Oscillation Near 200 cps.

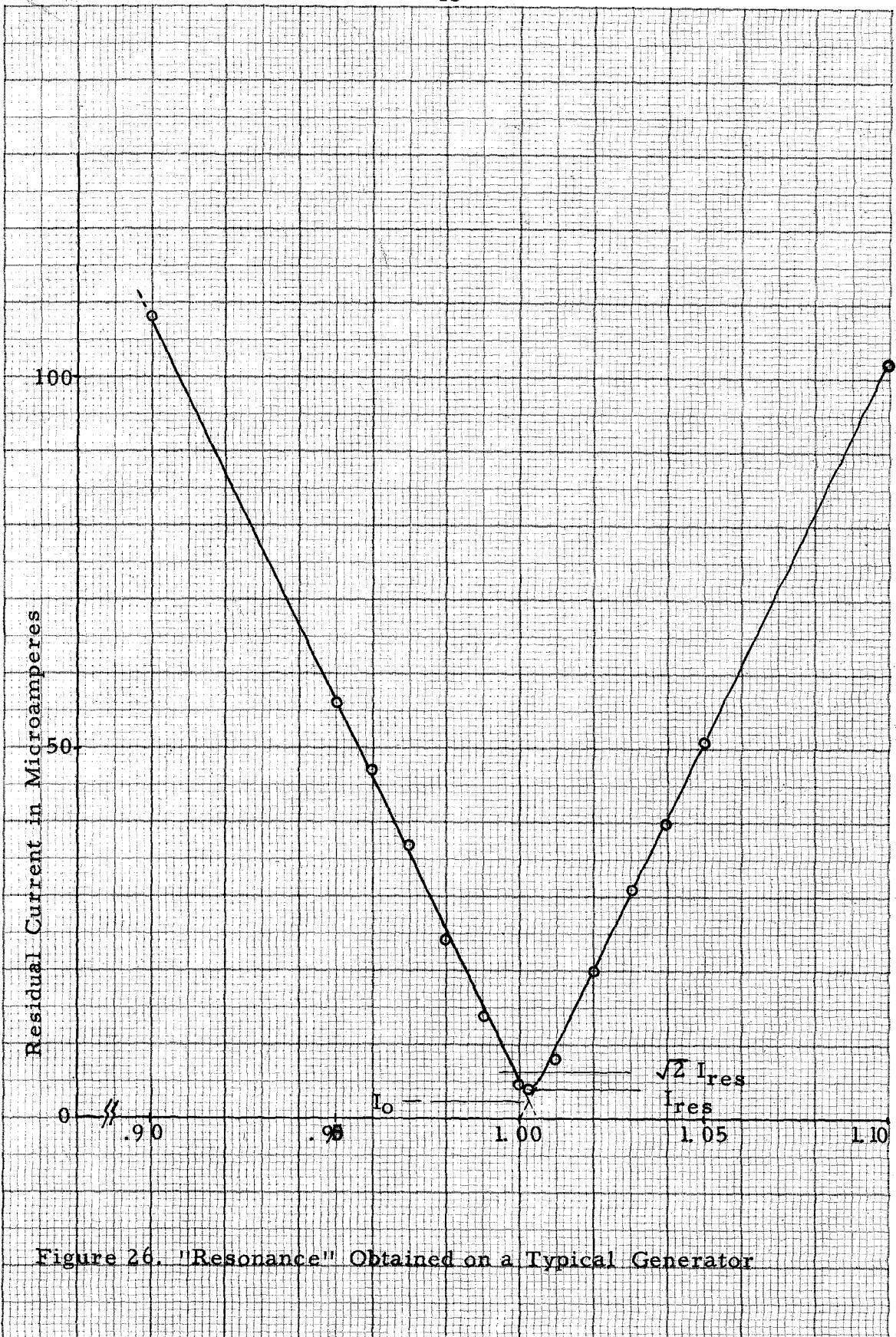


Figure 26. "Resonance" Obtained on a Typical Generator

amplifier. From this curve one may calculate a quality figure equivalent to the  $Q$  of a conventional reactance resonant circuit. This may be done by taking as the definition of  $Q$

$$Q = \frac{\omega_0}{\Delta\omega} \quad , \quad (\text{IV-17})$$

where  $\omega_0$  is the resonant frequency and  $\Delta\omega$  is the band width at the point where the current is  $\sqrt{2}$  times that at resonance (Ref. 25, pg 138). On this basis the  $Q$  of a typical amplifier is 250 at  $\lambda = 1.0$ .

An alternative formula, easily derived from the above is

$$Q = \frac{\lambda_0}{(\sqrt{2} - 1) I_0} \cdot \frac{\partial I}{\partial \lambda} \quad (\text{IV-18})$$

where  $\lambda = \omega^2$  and  $I_0$  is the minimum obtained by extrapolating the linear slopes. On this basis the  $Q$  is 960 at  $\lambda = 1.003$ .

The difference in  $Q$  as calculated by (IV-17) and (IV-18) is due to the residual out of phase components and noise pickup (mostly supply frequency in these amplifiers). It is felt by the author that the value of  $\lambda$  obtained by extrapolating the linear slopes is the more accurate.

Several views of the six-generator computer constructed by the author are shown in Figures 27 through 29. The panel is shown in Figure 27. The lower six pairs of terminals are the terminals of the generators. The actual value of negative conductance is determined by plug-in resistances, one of which is shown. The value of  $\lambda$  is set on the dial in the center of the panel. A rear view of the chassis is shown in Figure 28. Each set of four tubes in a row constitutes one

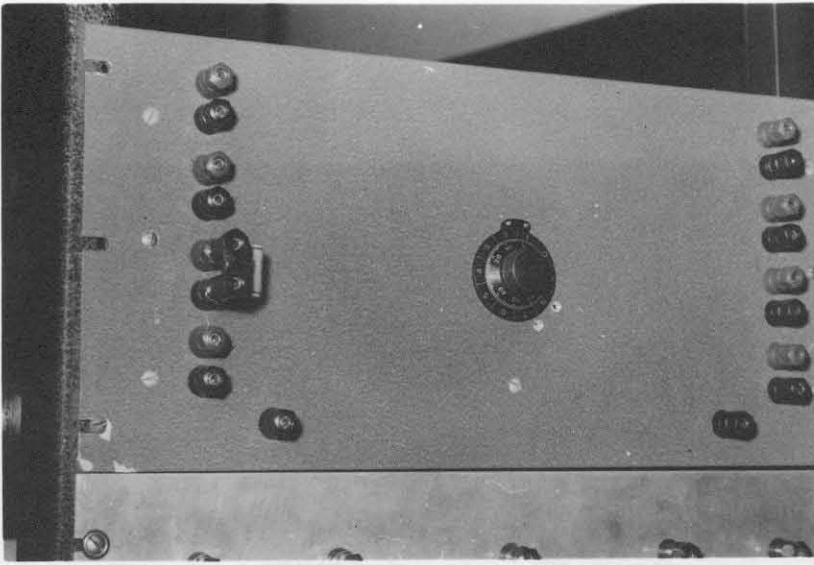


Figure 27. Six Generator Computer - Front Panel

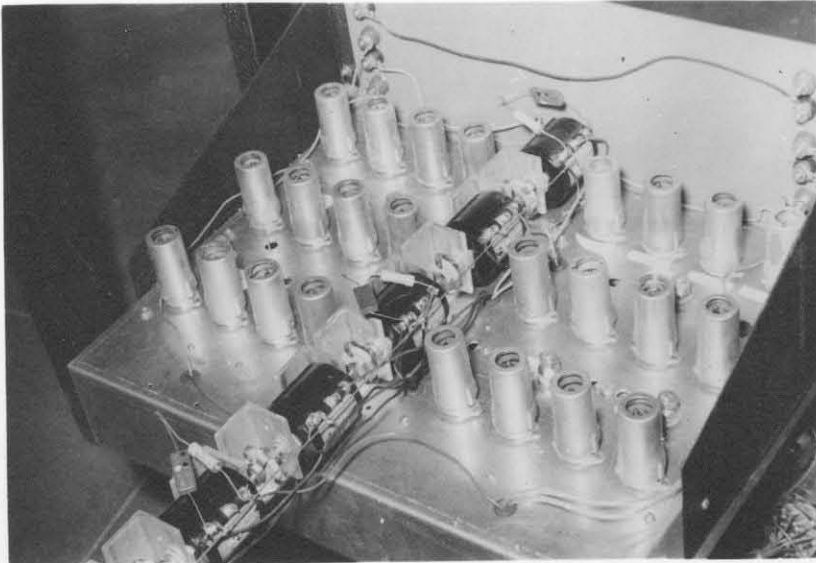


Figure 28. Six Generator Computer - Rear View

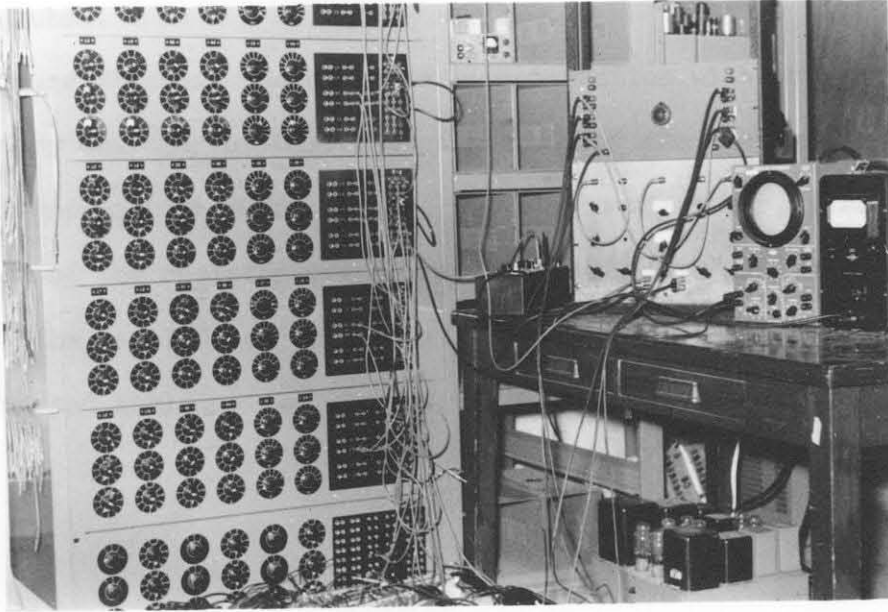


Figure 29. Computer in Operation - Plate Analog



generator. The  $\lambda$  potentiometers, connected by flexible couplings, are mounted on a piece of aluminum angle fastened to the chassis. Fine gain and phase shift adjustments are visible just behind the first row of tubes.

Figure 28 shows the computer in conjunction with the servomechanisms laboratory computer at CalTech, connected for the analog of section 5.5. Some of the many transformers are visible on the floor, while others and most of the resistors used are available at terminals on the plug board. The panel below the computer contains switches and shunts for metering and applying the constraints to the circuit.

## V. RESULTS OF TESTS ON ANALCGS

This portion of the thesis is concerned with the accuracy of the computer constructed by the author in determining the eigenvalues and eigenfunctions of several types of analog. The three circuits selected are the analogs for torsional vibration of a rod, bending of a beam, and the bending of a plate. Theoretical values for the results were calculated for comparison. In addition, two numerical examples are given to illustrate points brought out in the previous discussion.

### 5.1 Computation of the Eigenvalues and Eigenvectors of a Simple System

The configuration to be considered is the mass-spring system of figure 30, which is the lumped parameter mechanical analog for the torsional vibration of a uniform rod (see section 5.3). For this case  $M = E_5$  and

$$K = \begin{bmatrix} 3 & -1 & 0 & 0 & 0 \\ -1 & 2 & -1 & 0 & 0 \\ 0 & -1 & 2 & -1 & 0 \\ 0 & 0 & -1 & 2 & -1 \\ 0 & 0 & 0 & -1 & 1 \end{bmatrix} .$$

The determinantal equation is

$$|K - \lambda M| = 2 - 25\lambda + 50\lambda^2 - 35\lambda^3 + 10\lambda^4 - \lambda^5 = 0.$$

Thus the eigenvalues are

$$\lambda_1 = .098$$

$$\lambda_2 = .824$$

$$\lambda_3 = 2.000$$

$$\lambda_4 = 3.176$$

$$\lambda_5 = 3.902 .$$

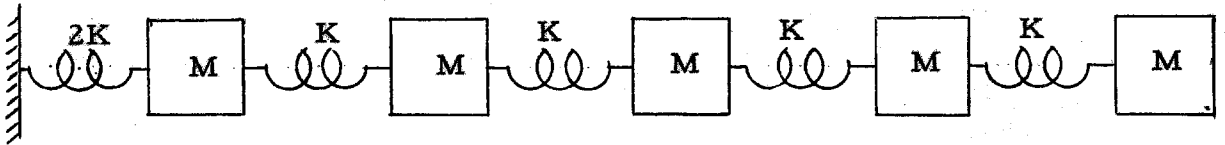


Figure 30. Lumped Mechanical Analog of Uniform Rod in Torsion

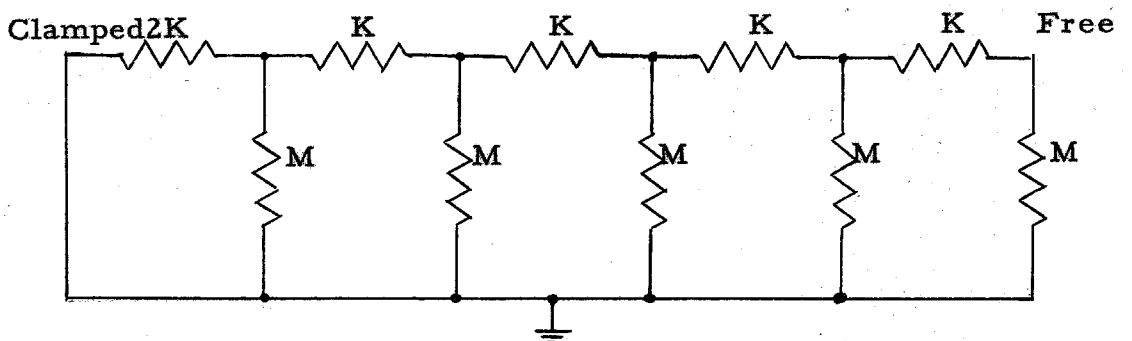


Figure 31. Electric Analog For Uniform Rod in Torsion

The normalized eigenvector matrix, A, is

$$A = \begin{bmatrix} .0989 & .2871 & .4472 & .5635 & .6247 \\ .2871 & .6247 & .4472 & -.0989 & -.5635 \\ .4472 & .4472 & -.4472 & -.4472 & .4472 \\ .5635 & -.0989 & -.4472 & .6247 & -.2871 \\ .6247 & -.5635 & .4472 & -.2871 & .0989 \end{bmatrix} .$$

It is easily verified that  $A^t M A = E_5$  and  $A^t K A = D(\lambda_1)$ .

## 5.2 Example of Stationary Power Input

Consider the following equation, representative of a 4-1/2 cell cantilever beam (section 5.4):

$$\begin{bmatrix} 7 - \lambda & -4 & 1 & 0 \\ -4 & 6 - \lambda & -4 & 1 \\ 1 & -4 & 5 - \lambda & -2 \\ 0 & 1 & -2 & 1 - \lambda \end{bmatrix} \begin{bmatrix} V_1 \\ V_2 \\ V_3 \\ V_4 \end{bmatrix} = \begin{bmatrix} I_1 \\ I_2 \\ I_3 \\ I_4 \end{bmatrix} . \quad (V - 1)$$

As indicated, four constraints are considered to be applied.

Establishing  $V_1$  as the fixed constraint, it is seen that definiteness of the matrix

$$\begin{bmatrix} 6 - \lambda & -4 & 1 \\ -4 & 5 - \lambda & -2 \\ 1 & -2 & 1 - \lambda \end{bmatrix} \quad (V - 2)$$

must be established if the driving power is to be an extreme value when the circuit is balanced (Section 3.4). Definiteness or non-definiteness of the matrix may be established by examination of its discriminants. If all are positive, the matrix is positive definite and the stationary point is a minimum. A similar rule holds for negative definiteness in the case of a maximum (Ref. 10, pg. 107).

The discriminants of the matrix (V - 2) are:

$$\begin{vmatrix} 6 & -\lambda & -4 & 1 \\ -4 & 5 & -\lambda & -2 \\ 1 & -2 & 1 & -\lambda \end{vmatrix} = (0.0516 - \lambda)(1.936 - \lambda)(10.013 - \lambda),$$

$$\begin{vmatrix} 6 & -\lambda & -4 \\ -4 & 5 & -\lambda \end{vmatrix} = (1.469 - \lambda)(9.531 - \lambda),$$

$$\begin{vmatrix} 6 & -\lambda & 1 \\ 1 & 1 & -\lambda \end{vmatrix} = (0.8075 - \lambda)(6.193 - \lambda),$$

$$\begin{vmatrix} 5 & -\lambda & -2 \\ -2 & 1 & -\lambda \end{vmatrix} = (5.828 - \lambda)(0.172 - \lambda),$$

(6 -  $\lambda$ ), (5 -  $\lambda$ ), and (1 -  $\lambda$ ).

The eigenvalues are

$$\lambda_1 = .02966$$

$$\lambda_2 = .98011$$

$$\lambda_3 = 5.5167$$

$$\lambda_4 = 12.475 .$$

It is seen that the discriminants are all positive for  $\lambda < .0516$  so that for these values of  $\lambda$  a power minimum may be obtained. Further inspection shows that for no value of  $\lambda > .0516$  are all the discriminants of the same sign, so that a power minimum cannot be achieved for this range of  $\lambda$ .

### 5.3 Torsional Vibration of a Rod

The differential equation for the torsional vibration of a rod is (Ref. 26, pg. 318)

$$\frac{\partial}{\partial x} \left\{ GI \frac{\partial \psi}{\partial x} \right\} = \rho I \frac{\partial^2 \psi}{\partial t^2} \quad (V - 3)$$

where  $\rho$  = density  
 $G$  = shear modulus of elasticity  
 $I$  = polar moment of inertia  
 $\psi$  = angular deflection.

Separating the variables as indicated in section 2.1, and using the finite difference approximation for the space derivative we have (using a uniform rod for simplicity)

$$\frac{\psi_{n-1} - 2\psi_n + \psi_{n+1}}{(\Delta x)^2} = - \frac{\omega^2 \rho \psi_n}{G} . \quad (V - 4)$$

The combination of variables  $\omega^2 (\Delta x)^2 \rho / G$  may be replaced by the eigenvalue variable  $\lambda$ . The equations for the transverse vibrations of a stretched string are of the same form with  $\lambda = \omega^2 (\Delta x)^2 \rho / T$ , where  $T$  is the tension on the string. An electric circuit which satisfies (V - 4) is shown in figure 31. Here a particular case has been assumed; it is that of a uniform rod approximated by five sections, one end being clamped and the other free.

It can easily be shown by substitution that a solution to (V - 4) is

$$\begin{aligned} \psi_n &= \text{Sin } (2n - 1)\beta_k \\ \lambda_k &= 4\text{Sin}^2 \beta_k \end{aligned} \quad (V - 5)$$

where  $\beta_k = (2k-1)\pi/4N$ ,  $k$  being the eigenvalue index and  $N$  the number of sections. This equation serves as a basis for the theoretical calculations which are compared in table V-1 with the results obtained on the computer. The experimentally obtained eigenvectors are plotted in figure 32.

TABLE V - 1

## TORSIONAL VIBRATION OF A UNIFORM CANTILEVER ROD

Five Cell Analog						
Mode	1		2		3	
Calculated $\lambda$	.098		.824		2.00	
Experimental $\lambda$	.098		.818		1.98	
Normalized Eigenvectors						
Station	calc	exp	calc	exp	calc	exp
1	.0989	.095	.2871	.289	.4472	.395
2	.2871	.286	.6247	.585	.4472	.460
3	.4472	.450	.4472	.470	-.4472	-.451
4	.5635	.563	-.0989	-.097	-.4472	-.470
5	.6247	.625	-.5635	-.586	.4472	.455

Figure 33, showing the measured input current at the fixed constraint for  $\lambda$ 's near the system eigenvalues, illustrates the sharpness of convergence. Successive values of  $\lambda$  chosen are indicated by the numbering of the points. Modes higher than the third would require all junctions to be constrained. This is due to the fact that leaving any single junction unconstrained leaves a region with lowest eigenvalue equal to  $\lambda_3$  (see section 3.4).

#### 5.4 Bending of a Beam

The differential equation for the bending of a beam is (Ref. 26, pg. 324)

$$\frac{\partial^2}{\partial x^2} \left[ EI \frac{\partial^2 y}{\partial x^2} \right] = -m \frac{\partial^2 y}{\partial t^2} \quad (V - 6)$$

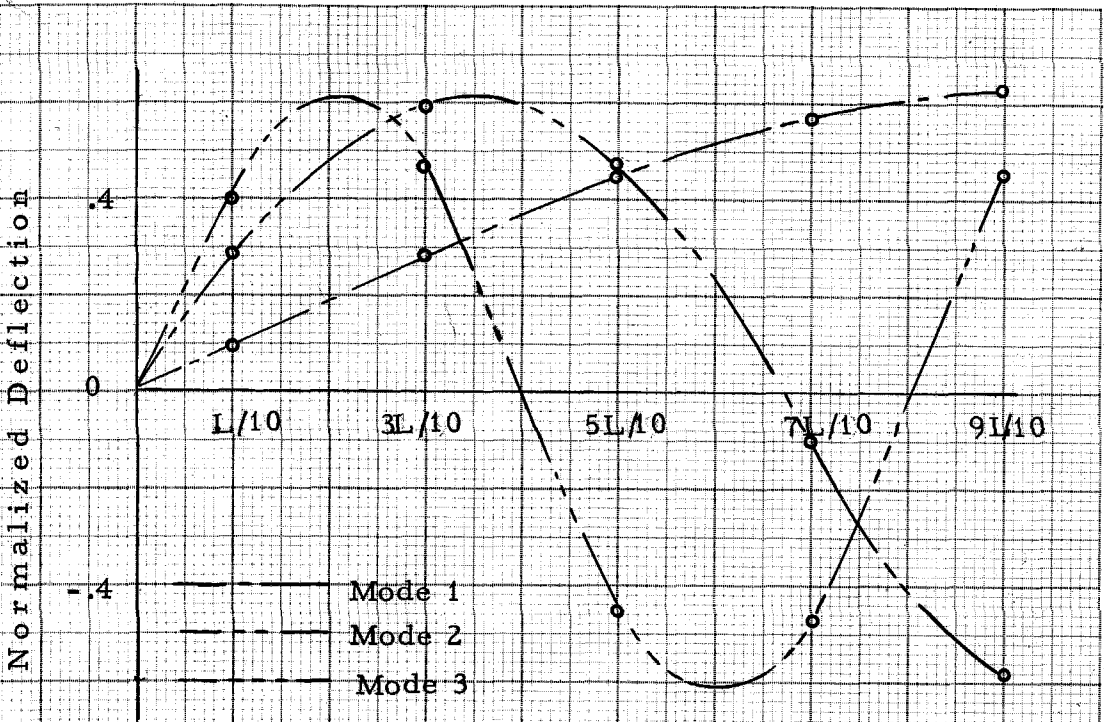


Figure 32. Normalized Eigenvectors for Uniform Rod in Torsion

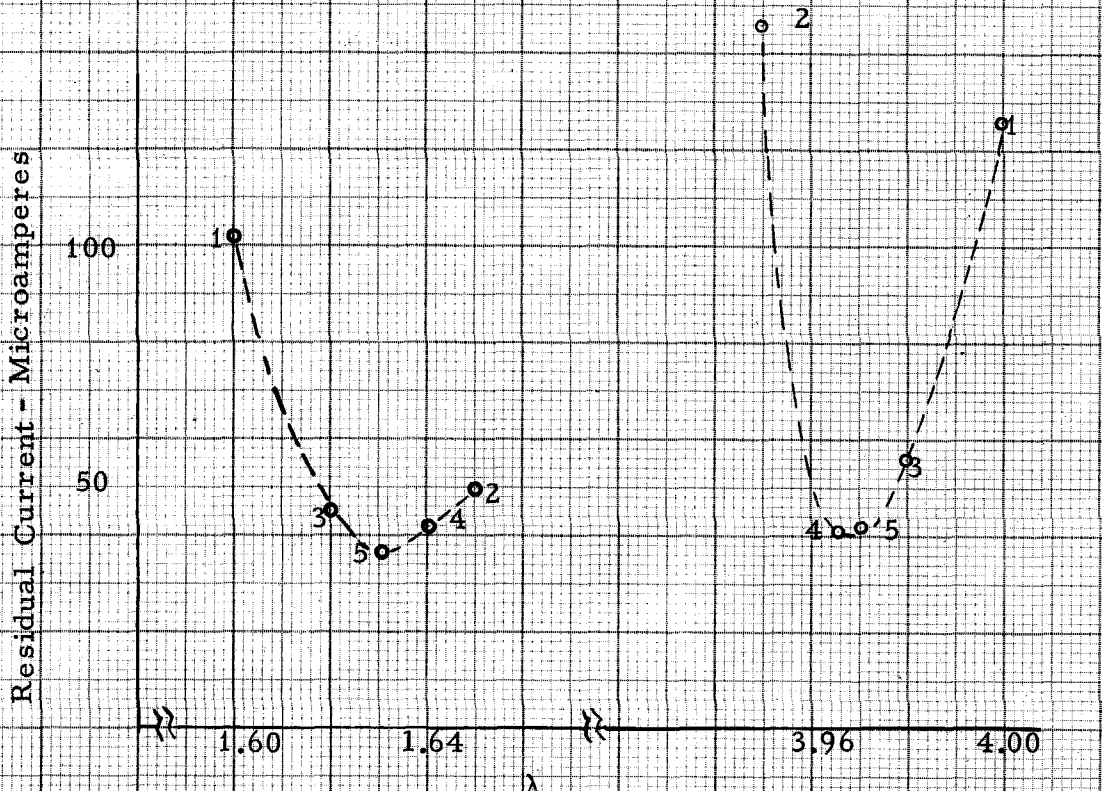


Figure 33. Convergence on Eigenvalues



where  $y$  = deflection of the neutral axis  
 $E$  = modulus of elasticity  
 $I$  = moment of inertia of cross section  
 $m$  = mass per unit length.

For a uniform beam, the finite difference form is

$$(y_{n-2} - 4y_{n-1} + 6y_n - 4y_{n+1} + y_{n+2}) = m\Delta x^4 \omega^2 y_n. \quad (V - 7)$$

An electric analog of this equation (Ref. 19) is shown in figure 4.

The particular case chosen is that of a uniform cantilever beam represented by 4-1/2 cells\*. This is the example used in section 5.2. The solution may be obtained numerically as outlined in sections 2.1 and 5.1. Table V-2 lists the calculated and experimental results for comparison, and the eigenvectors are plotted in figure 34.

TABLE V - 2

BENDING VIBRATION OF A UNIFORM CANTILEVER BEAM

Mode	1		2		3		4	
Calculated $\lambda$	.0297		.980		5.71		12.49	
Experimental $\lambda$	.03		.975		5.48		12.44	
Normalized Eigenvectors								
Station	calc	exp	calc	exp	calc	exp	calc	exp
1	.084	.083	-.403	-.406	.712	.714	-.571	-.610
2	.271	.275	-.693	-.689	.108	.115	.661	.636
3	.525	.527	-.341	-.342	-.625	-.626	-.469	-.453
4	.805	.800	.496	.495	.301	.293	.140	.129

\* A somewhat different analog circuit is presented in reference 16.

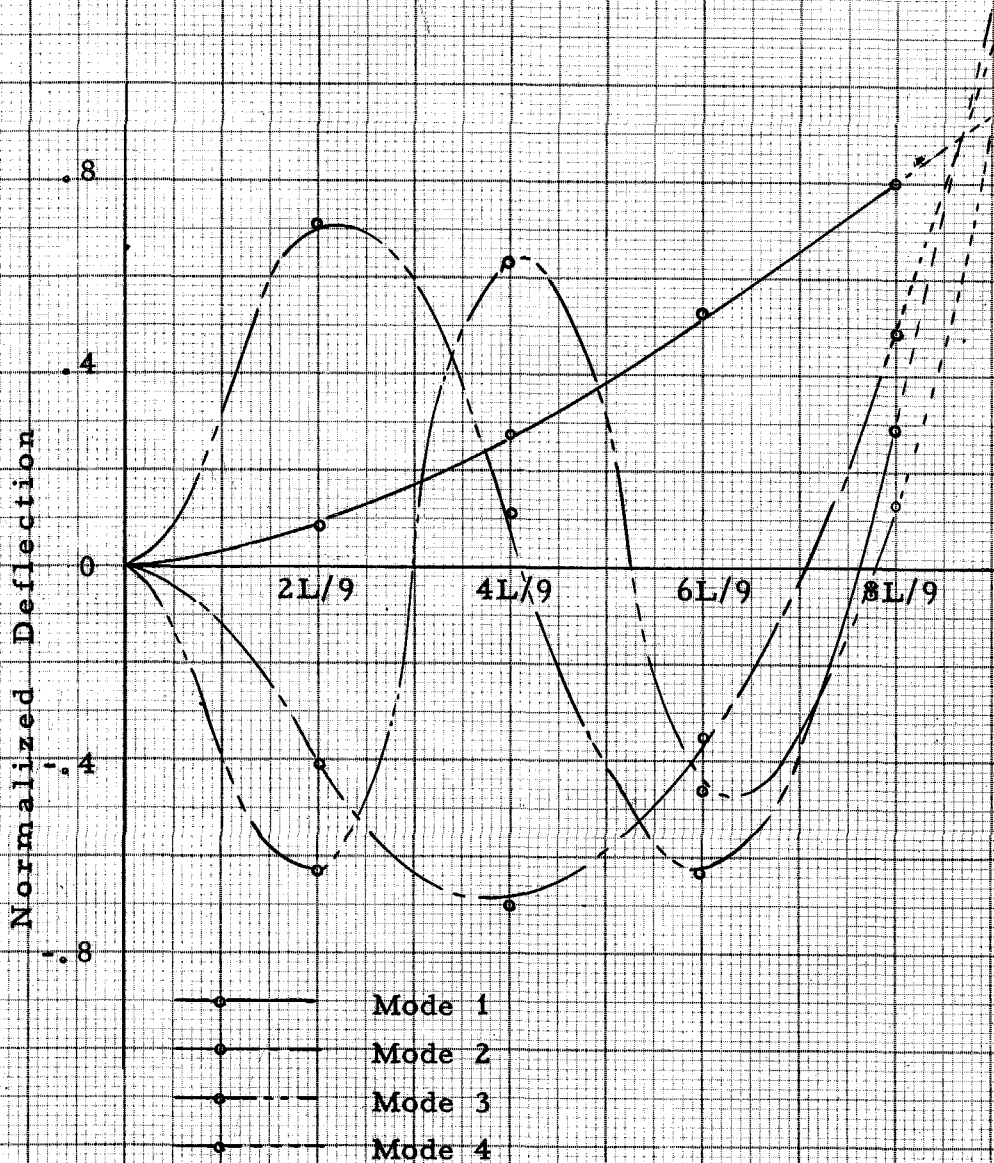


Figure 34. Normalized Eigenvectors for Uniform Cantilever Beam

An orthogonality check is made by taking the product  $A^t M A$ . The results (V-8) indicate an r.m.s. error of 1.4% due mostly to inaccuracies in the highest mode.

$$A^t M A = \begin{bmatrix} .083 & .275 & .528 & .799 \\ -.406 & -.688 & -.341 & .495 \\ .713 & .115 & -.626 & .293 \\ -.606 & .645 & -.447 & .130 \end{bmatrix} \begin{bmatrix} .083 & -.406 & .713 & -.606 \\ .275 & -.688 & .115 & .645 \\ .528 & -.341 & -.626 & -.447 \\ .799 & .495 & .293 & .130 \end{bmatrix}$$

$$\begin{bmatrix} .9497 & & & \\ & .9995 & & \\ & & .9993 & \\ & & & 1.0000 \end{bmatrix} \quad (V-8)$$

(Symmetric)

Four constraints were required in obtaining the third and fourth modes. In the balanced condition, the residual currents with  $\lambda = \lambda_3$  and  $\lambda = \lambda_4$  ranged from 8 to 100 microamperes. About one hour was required to converge on mode 3, while only 30 minutes were taken in finding mode 4.

### 5.5 Bending of a Plate.

The final example chosen is that of the bending vibration of a square cantilever plate. This problem was selected as an example of a partial differential equation with two space variables, and for the large number of transformers required. It was felt that this circuit constituted a rather severe test of the computer's capability for handling parasitics and low impedances.

The general differential equation for the bending of a plate is (Ref. 25, pg. 441)

$$\frac{\partial^2}{\partial x^2} \left[ D \left( \frac{\partial^2 u}{\partial x^2} + \nu \frac{\partial^2 u}{\partial y^2} \right) \right] + \frac{\partial^2}{\partial y^2} \left[ D \left( \frac{\partial^2 u}{\partial y^2} + \nu \frac{\partial^2 u}{\partial x^2} \right) \right] + 2 \frac{\partial^2}{\partial x \partial y} \left[ D(1 - \nu) \frac{\partial^2 u}{\partial x \partial y} \right] = m \frac{\partial^2 u}{\partial t^2} \quad (V - 9)$$

where  $u$  = deflection of the plate

$$D = \frac{Eh^3}{12(1 - \nu^2)}, \text{ the flexural rigidity}$$

$m$  = mass per unit area

$\nu$  = Poisson's ratio

$h$  = thickness

$E$  = Young's modulus.

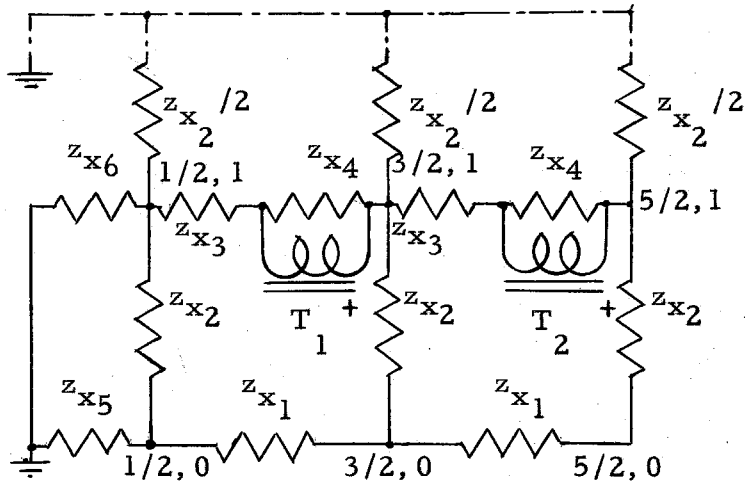
An alternative form of this equation is

$$\frac{\partial}{\partial y} \left\{ \frac{\partial}{\partial y} \left[ D \left( \frac{\partial^2 u}{\partial y^2} + \nu \frac{\partial^2 u}{\partial x^2} \right) \right] + \frac{\partial}{\partial x} \left[ D(1 - \nu) \frac{\partial^2 u}{\partial x \partial y} \right] \right\} + \frac{\partial}{\partial x} \left\{ \frac{\partial}{\partial x} \left[ D \left( \frac{\partial^2 u}{\partial x^2} + \nu \frac{\partial^2 u}{\partial y^2} \right) \right] + \frac{\partial}{\partial y} \left[ D(1 - \nu) \frac{\partial^2 u}{\partial x \partial y} \right] \right\} = m \frac{\partial^2 u}{\partial t^2} \quad (V - 10)$$

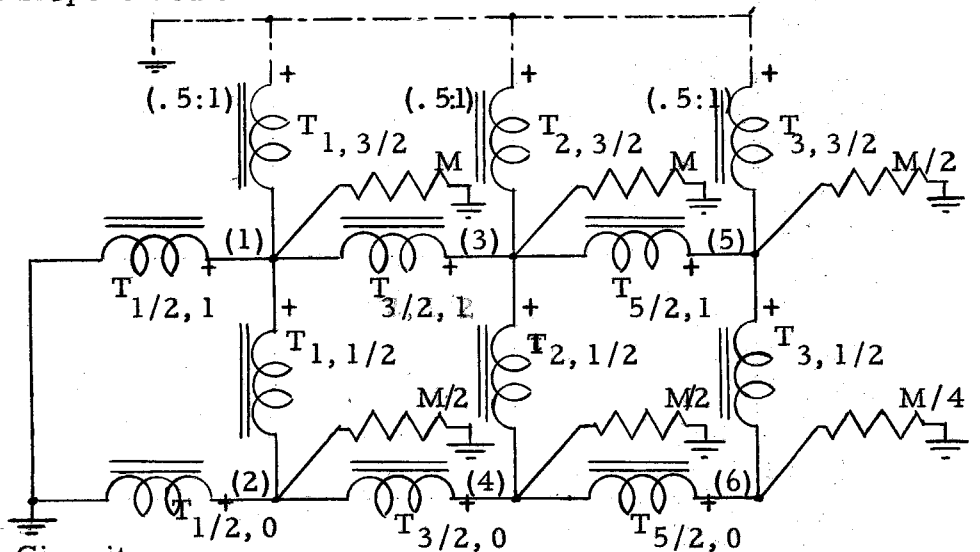
The circuit used\* is that of figures 35 and 36, which is for the case of a square cantilever plate represented by 12 cells. Symmetry considerations allow one to use only six negative conductance generators, as shown.

No analytical solution has been obtained for this circuit, so far as is known to the author. This case was solved by MacNeal (Ref. 4) and, for 18 degrees of freedom rather than 12, by Young (Ref. 27). Unfortunately, an error of about 2% in the value used by

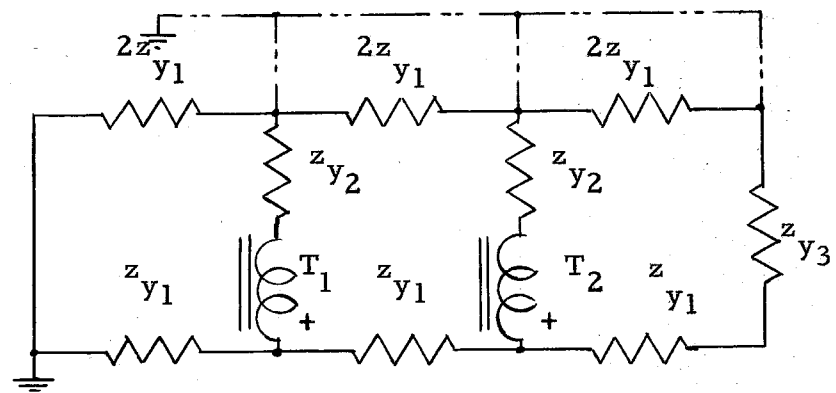
\* This analogy was developed by Dr. R. H. MacNeal (Refs. 4 and 19, pg 126). Non-uniform plates and beams and other boundary conditions are treated in detail in these references.



a) Horizontal Slope Circuit



b) Deflection Circuit



c) Vertical Slope Circuit

--- Connected for unsymmetric Modes  
 - - - - - Connected for symmetric modes

NOTE: Secondaries of transformers in deflection circuit are connected to corresponding junctions of slope circuits.

Figure 35. Electric Analog for Square Cantilever Plate

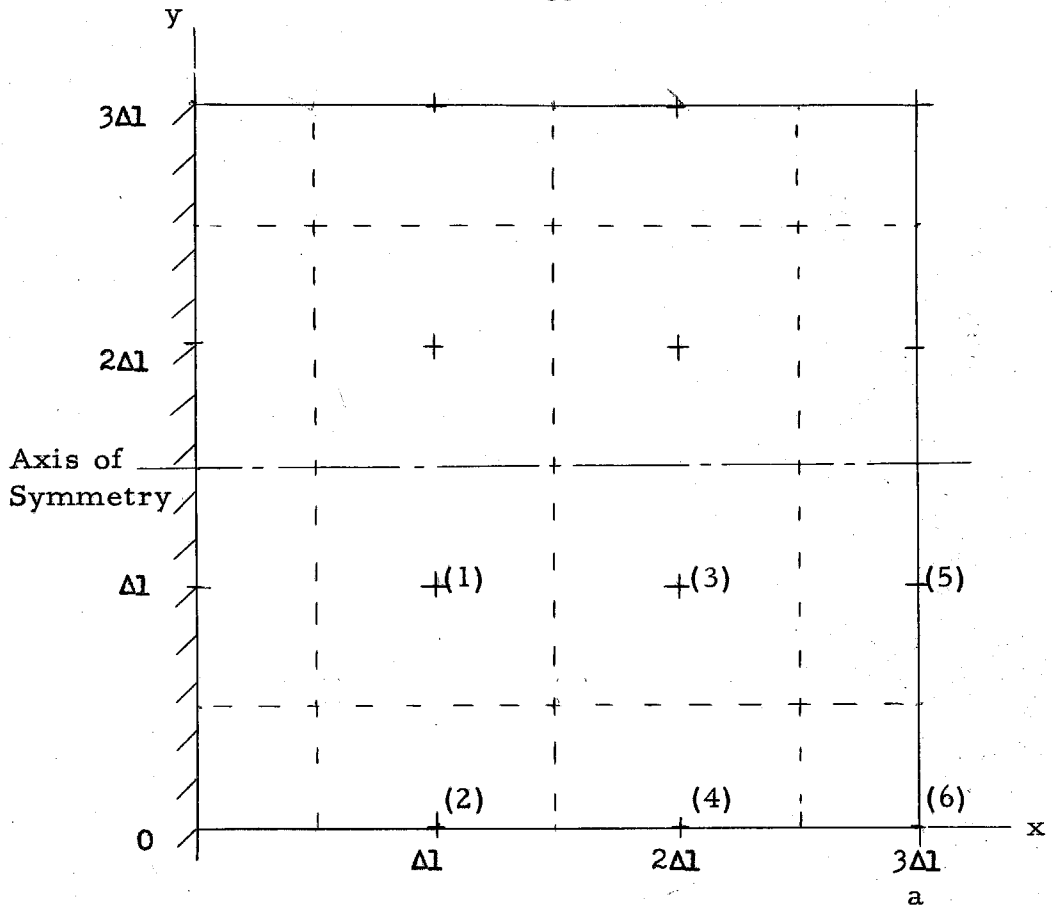


Figure 36. Square Cantilever Plate

TABLE V - 3

## IMPEDANCE VALUES FOR PLATE ANALOG

$$z_{x_1} = z_{y_3} = \frac{(1-\nu^2)}{2} \quad z_{x_4} = \frac{(1-\nu^2)}{2}$$

$$z_{x_2} = z_{y_1} = 1 - \nu \quad z_{x_5} = 1 - \nu^2$$

$$z_{x_3} = z_{y_2} = 1 + \nu \quad z_{x_6} = 2$$

the author for several of the impedances ( $z_{x_1}$ ,  $z_{x_5}$ ,  $z_{y_3}$ ) was discovered after the computer was dismantled, so that a direct comparison of results is impossible. It was possible, however, to set up the equations for the network of figure 35, and to solve them numerically for the eigenvalues and eigenvectors. The six resulting equations for both the symmetrical and unsymmetrical cases are given in V-11, page 67, where the upper signs refer to the symmetrical case. For clarity only the subscripts of the admittances are written. Thus, " $x_3 x_4$ " means " $(1/z_{x_3}) \cdot (1/z_{x_4})$ ", etc. The same equation, written in terms of Poisson's ratio,  $\nu$ , is also given (V-12).

$$\begin{bmatrix} 20 \mp 8 & -6+2\nu \pm 1 & -8 \mp 2 & 2-\nu & 1 & 0 \\ -6+2\nu \pm 1 & \frac{17-8\nu-7\nu^2}{2} & 2-\nu & -2(2+\nu)(1-\nu) & 0 & \frac{1-\nu^2}{2} \\ -8 \pm 2 & 2-\nu & 18 \mp 8 & -6+2\nu \pm 1 & -6+2\nu+(2-\nu) & 2(1-\nu) \\ 2-\nu & -2(2+\nu)(1-\nu) & -6+2\nu \pm 1 & \frac{15-8\nu-5\nu^2}{2} & 2-\nu & -(1-\nu)(3+\nu) \\ 1 & 0 & -6+2\nu \pm (2-\nu) & 2-\nu & \frac{15-8\nu-5\nu^2}{2} & -(3-\nu^2) \\ & & & & \mp(4-2\nu-2\nu^2) & \pm \frac{(1-4\nu-\nu^2)}{2} \\ 0 & \frac{(1-\nu^2)}{2} & 2(1-\nu) & -(1-\nu)(3+\nu) & -(3-\nu^2) & (1-\nu)(3+\nu) \\ & & & & \pm \frac{(1-4\nu-\nu^2)}{2} & \end{bmatrix}$$

$$-\lambda D(1, 1/2, 1, 1/2, 1/2, 1/4) = 0 \quad (\text{V} - 12)$$

$$\begin{array}{r}
 8x_2 + 10x_3 + x_6 \\
 \hline
 74(x_2 + x_3) \\
 \hline
 \frac{x_3}{2x_3 + x_4} \\
 \hline
 -2(2x_2 + x_3) \\
 \hline
 \frac{x_3(x_3 + x_4)}{2x_3 + x_4} \\
 \hline
 -2(2x_2 + 2x_3 + x_2) \\
 \hline
 \frac{x_3^2}{2x_3 + x_4} + 2x_2 \\
 \hline
 \frac{x_3(x_3 + x_4)}{2x_3 + x_4} \\
 \hline
 0
 \end{array}
 \left[ \begin{array}{r}
 0 \\
 x_1 \\
 2x_2 \\
 -2(x_1 + x_2) \\
 -2(x_1 + x_2) + x_1 \\
 2(x_1 + x_2)
 \end{array} \right]$$

$$\begin{array}{r}
 5x_1 + 4x_2 + x_3 + x_5 \\
 \hline
 \frac{x_3}{2x_3 + x_4} \\
 \hline
 2x_2 + x_3 \\
 \hline
 -2(2x_1 + x_2) \\
 \hline
 8x_2 + 9x_3 + x_4 \\
 \hline
 \frac{x_3(x_3 + x_4)}{2x_3 + x_4} \\
 \hline
 74(x_2 + x_3) \\
 \hline
 \frac{x_4(x_3 + x_4)}{2x_3 + x_4} \\
 \hline
 -2(2x_2 + x_3) \\
 \hline
 \frac{x_3(x_3 + x_4)}{2x_3 + x_4} \\
 \hline
 -2(2x_2 + x_3) \\
 \hline
 \frac{x_3(x_3 + x_4)}{2x_3 + x_4} \\
 \hline
 7(2x_2 + x_3) \\
 \hline
 \frac{x_3(x_3 + x_4)}{2x_3 + x_4} \\
 \hline
 -2(2x_2 + x_3) \\
 \hline
 \frac{x_3(x_3 + x_4)}{2x_3 + x_4} \\
 \hline
 2x_2 + x_3 \\
 \hline
 \frac{x_3(x_3 + x_4)}{2x_3 + x_4} \\
 \hline
 5x_1 + 4x_2 + x_3 \\
 \hline
 \frac{x_3^2}{2x_3 + x_4} \\
 \hline
 -2(x_1 + x_2) \\
 \hline
 5x_1 + 4x_2 + x_3 + x_4 \\
 \hline
 \frac{(x_3 + x_4)^2}{2x_3 + x_4} \\
 \hline
 72(2x_1 + x_2) \\
 \hline
 \frac{(x_3 + x_4)^2}{2x_3 + x_4} \\
 \hline
 2(x_1 + x_2)
 \end{array}$$

(symmetric)

(V - II)

$$-\lambda D(1, 1/2, 1, 1/2, 1/2, 1/4) = 0$$



Taking  $\nu = 0.3$ , the correct equations are

$$\begin{bmatrix} 12.0 & -4.4 & -6.0 & 1.7 & 1.0 & 0.0 \\ -8.8 & 13.97 & 3.4 & -6.44 & 0.0 & 0.91 \\ -6.0 & 1.7 & 10.0 & 4.40 & -3.7 & 1.4 \\ 3.4 & -6.44 & -8.8 & 12.15 & 3.4 & -4.62 \\ 2.0 & 0.0 & -7.4 & 3.4 & 5.71 & -3.71 \\ 0.0 & 1.82 & 5.6 & -9.24 & -7.42 & 9.24 \end{bmatrix}$$

$$-E_6 \lambda_s = 0 \quad (V-13)$$

and

$$\begin{bmatrix} 28.00 & -6.40 & -10.00 & 1.70 & 1.00 & 0.00 \\ -12.80 & 13.97 & 3.40 & -6.44 & .00 & .91 \\ -10.00 & 1.70 & 26.00 & -6.40 & -7.10 & 1.40 \\ 3.40 & -6.44 & -12.80 & 12.15 & 3.40 & -4.62 \\ 2.00 & 0.00 & -14.20 & 3.40 & 18.59 & -5.53 \\ 0.00 & 1.82 & 5.60 & -9.24 & -11.06 & 9.24 \end{bmatrix}$$

$$-E_6 \lambda_u = 0 \quad (V-14)$$

where the subscripts S and U indicate the symmetrical and unsymmetrical cases respectively. The erroneous values used were

$$z_{x1} = 2.25 \text{ vice } 2.2,$$

$$z_{x5} = 1.125 \text{ vice } 1.1,$$

$$z_{y3} = 2.25 \text{ vice } 2.2.$$

Use of these values leads to the equations

$$\begin{bmatrix} 11.9900 & -4.3956 & -5.9941 & 1.6983 & 0.9990 & 0.0000 \\ -8.7912 & 13.8146 & 3.3966 & -6.3527 & 0.0000 & 0.8888 \\ -5.9941 & 1.6983 & 9.9900 & -4.3956 & -3.6930 & 1.3986 \\ 3.3966 & -6.3527 & -8.7912 & 12.0368 & 3.3966 & -4.5749 \\ 1.9980 & 0.0000 & -7.3860 & 3.3966 & 5.6880 & -3.6860 \\ .0000 & 1.7776 & 5.5944 & -9.1499 & -7.3721 & 9.1499 \end{bmatrix}$$

$$-E_6 \lambda_s = 0 \quad (V-15)$$

$$\begin{bmatrix} 27.9772 & -6.3936 & -9.9900 & 1.6983 & 0.9990 & 0.0000 \\ -12.7872 & 13.8146 & 3.3966 & -6.3527 & 0.0000 & 0.8888 \\ -9.9900 & 1.6983 & 25.9772 & -6.3936 & -7.0929 & 1.3986 \\ 3.3966 & -6.3527 & -12.7872 & 12.0368 & 3.3966 & -4.5749 \\ 1.9980 & 0.0000 & -14.1858 & 3.3966 & 18.3896 & -10.9277 \\ 0.0000 & 1.7776 & 5.5944 & -9.1499 & -10.9277 & 9.1499 \end{bmatrix}$$

$$-E_6 \lambda_u = 0 \quad (V-16)$$

The eigenvalues obtained are compared in Table V-4. The normalized eigenvectors obtained experimentally are given in Table V-5. Contour lines showing the mode shapes obtained are plotted in figure 37. These are a good example of the principles on the nodes of eigenfunctions described in 2.3.

TABLE V - 4

## EIGENVALUES FOR SQUARE CANTILEVER PLATE

$$\lambda_k = \frac{\omega_k^2 \Delta l^4_m}{D} = \frac{\omega_k^2 a^4_m}{81D}$$

$\nu = 0.3$ , 12 cells (figures 35, 36)

k	Symmetry	Eigenvalues		
		Calculated (z's used)	Experimental	MacNeal* (Ref. 4)
1	S	0.1242	0.129	0.124
2	U	0.6422	0.640	0.616
3	S	2.5840	2.44	2.38
4	S	4.4221	4.32	3.96
5	U	5.7432	5.75	5.30

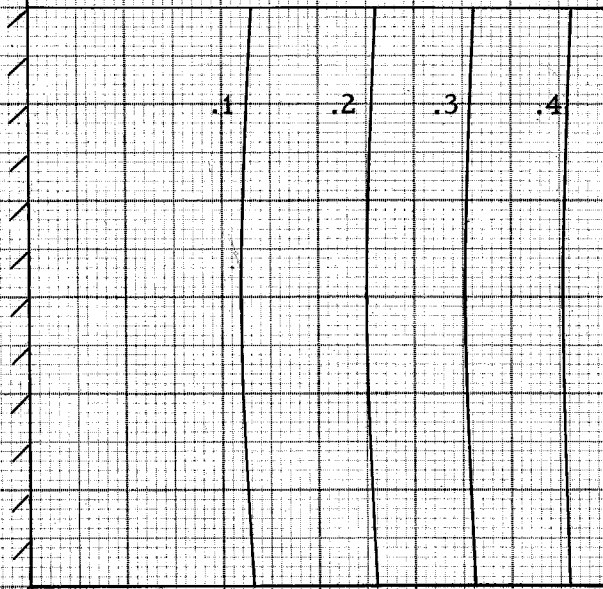
TABLE V - 5

## NORMALIZED EIGENVECTORS FOR SQUARE CANTILEVER PLATE\*\*

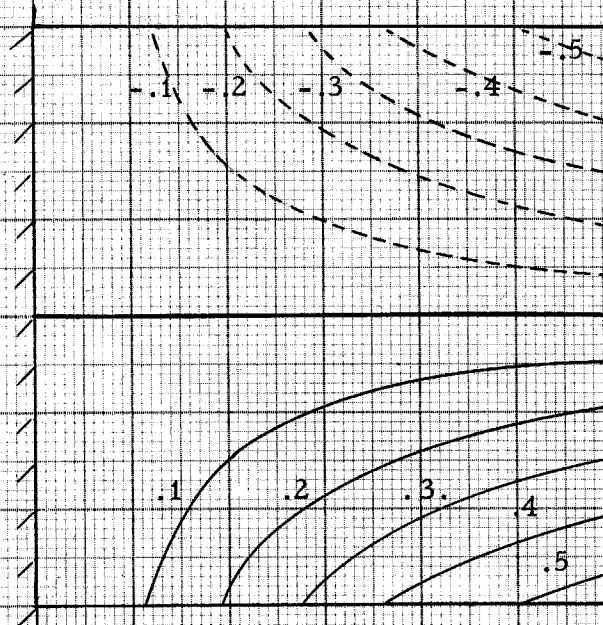
Station	Mode				
	1	2	3	4	5
1	.082	.066	-.223	-.182	-.148
2	.074	.205	-.321	.091	-.427
3	.249	.149	-.146	-.220	-.060
4	.242	.426	-.336	.349	-.230
5	.448	.213	.365	-.203	.252
6	.440	.597	.153	.576	.548

\* These values are  $f_M^2 (4\pi^2 / 81)$  where  $f_M$  is the frequency given by MacNeal.

\*\* The values for the other six stations may be obtained by symmetry.

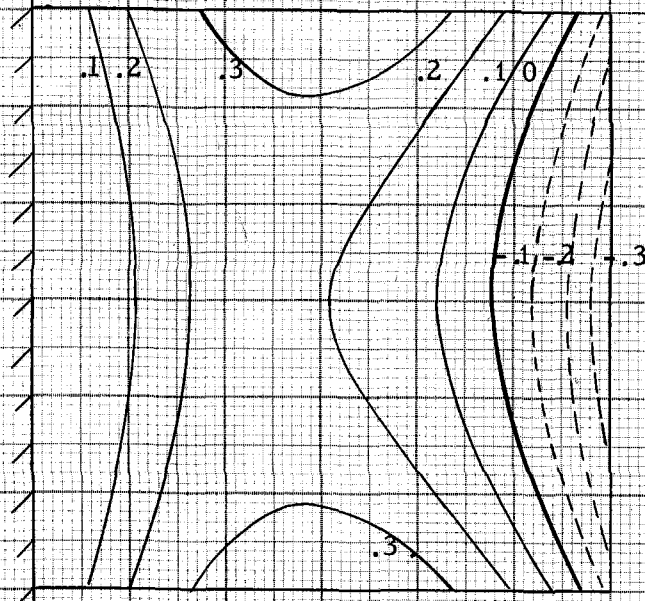


$$\lambda_1 = .1242$$

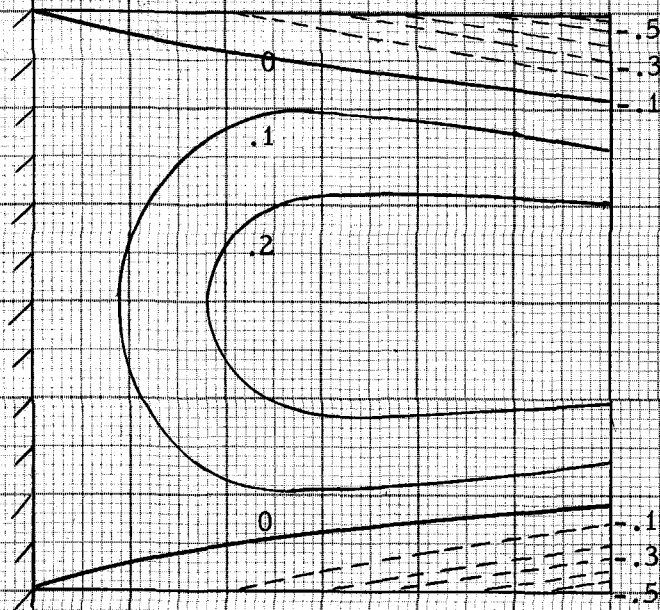


$$\lambda_2 = .6422$$

Figure 37. Normalized Eigenvectors for Square Cantilever Plate

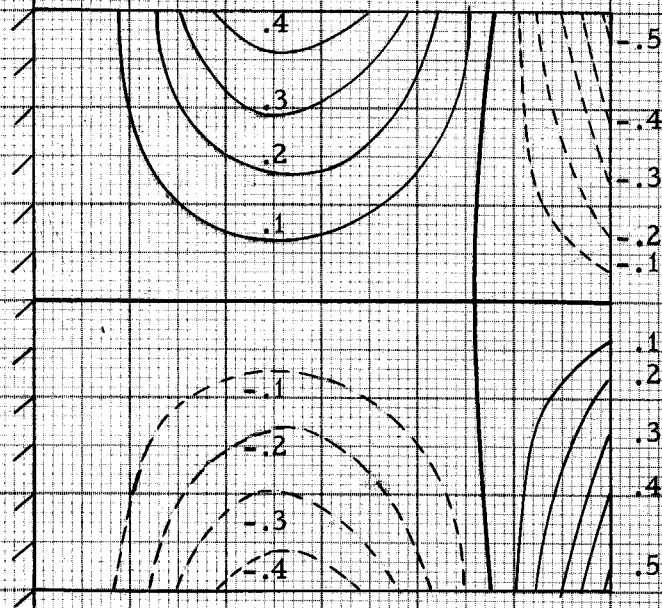


$\lambda_3 = 2.584$



$\lambda_4 = 4.422$

Figure 37. (Continued) Normalized Eigenvectors for Square Cantilever Plate



$$\lambda_5 = 5.7432$$

Figure 37 (Continued). Normalized Eigenvectors for Square Cantilever Plate

## VI. DISCUSSION AND CONCLUSION

This work has been directed toward the development of a computer suitable for the solution of various eigenvalue problems. The problems solved are of a type suitable for solution with direct electric analogs, using pure reactance networks. By employing resistors and positive-gain amplifiers as computing elements, costly high precision inductances and capacitors may be eliminated. This substitution is not without disadvantages, however, for such a computer is not suitable for the solution of transient problems. Also, the interconnection of many active elements causes undesired oscillations which must be suppressed when determining eigenvalues and eigenvectors.

The majority of this work has been concerned with methods of suppressing these oscillations. Methods based on the known properties of eigenvectors have proved suitable for determining driving points and for obtaining convergence to normal modes.

The computer constructed for the tests of Part V has some disadvantages. The most severe was associated with the low output impedance and peak voltage capacity of the final amplifier of the negative conductance generators. This could be most easily corrected, no doubt, by use of a direct-coupled amplifier and a somewhat different output amplifier. Some advantage might be gained by using a higher working frequency. No effort was made in this direction by the author, due to the lower frequency design of the available transformers.

A more positive method of achieving convergence at a normal mode

based on minimizing on error magnitude, has been indicated (section 3.4). The construction of such a system, and the elimination of the limitations of the output circuit should provide a computer capable of high accuracy with a reasonable amount of effort and expense.

In summary

- i) An electric analog involving interconnected negative conductance generators will break into spontaneous oscillations when the equivalent frequency is at least equal to the lowest normal mode frequency.
- ii) Suppression of this oscillation and the determination of higher normal mode frequencies and mode shapes requires the addition of constraints. At least one additional constraint must be added for each successive mode.
- iii) A computer of reasonable accuracy (1%) may be constructed using R-C coupled amplifiers, resistors, and transformers.



## REFERENCES

1. Kron, G.: "Electric Circuit Models of Partial Differential Equations", Elec. Eng., V. 67, pp 672-684, July 1948.
2. Pipes, L. A.: "Electrical Circuit Analysis of Torsional Oscillations", Jour. App. Physics, V.14, No. 7, pp357-62, July 1943.
3. McCann, G. D. and R. H. MacNeal: "Beam Vibration Analysis with the Electric Analog Computer", Jour. of App. Mechanics, (Trans. ASME) V. 17, pp 13-26, 1950.
4. MacNeal, R. H.: "Solution of Elastic Plate Problems by Electric Analogies", Jour. of App. Mechanics, V. 18, No. 1, pp 59-67, March 1951.
5. Wilts, C. H. and G. D. McCann: "New Electric Analog Computers and Their Application to Aircraft Design Problems", Analysis Laboratory, California Institute of Technology.
6. Liebmann, G.: "Solution of Partial Differential Equations with a Resistance Network Analogue", British Journ. App. Physics, V. 1, No. 4, pp 92-103, April 1950.
7. Swenson, G. W. Jr.: "A D.C. Network Analyzer for Solving Wave-Equation Boundary Value Problems", PhD Thesis, University of Wisconsin, 1951.
8. Swenson, G. W. Jr., and T. J. Higgins: "A Direct Current Network Analyzer for Solving Wave-Equation Boundary-Value Problems", Jour. App. Physics, V. 23, No. 1, pp 126-131, January 1952.
9. Swenson, G. W. Jr: "Analysis of Non-Uniform Columns and Beams by a Simple D. C. Network Analyzer", Jour. Aero. Sci., V. 19, No. 4, pp 273-275, April 1952.
10. Perlis, Sam: "Theory of Matrices", Addison Wesley Press, Cambridge, Mass., 1952.
11. Crumb, S. F.: "A Study of the Effects of Damping on Normal Modes of Electrical and Mechanical Systems", PhD Thesis, California Institute of Technology, 1955.
12. Frazer, R. A., W. J. Duncan and A. R. Collar: "Elementary Matrices and Some Applications to Dynamics and Differential Equations", Cambridge University Press, 1950.

13. Courant, R. and Hilbert, D.: "Methods of Mathematical Physics", V. I, Interscience Press, New York, 1953.
14. Rayleigh, Baron (J. W. Strutt): "Theory of Sound", Dover, New York, 1945, (reprint of 2nd Edition of 1894).
15. Gardner, M. F. and Barnes, J. F.: "Transients in Linear Systems", John Wiley and Sons, New York, 1947.
16. Russell, W. T.: "Lumped Parameter Analogies for Continuous Mechanical Systems", PhD Thesis, California Institute of Technology, 1950.
17. Bode, H. W.: "Network Analysis and Feedback Amplifier Design", D. Van Nostrand Co., New York, 1945.
18. Southwell, R. V.: "Relaxation Methods in Theoretical Physics", The Clarendon Press, Oxford, 1946.
19. MacNeal, R. H.: "The Solution of Partial Differential Equations by Means of Electrical Networks", PhD Thesis, California Institute of Technology, 1949.
20. Murray, F. J.: "The Theory of Mathematical Machines", King's Crown Press, New York, 1948.
21. Walker, R. M.: "An Analog Computer for the Solution of Linear Simultaneous Equations", Proc. I. R. E., V. 37, No. 12, pp 1467-1473, December 1949.
22. Courant, R.: "Differential and Integral Calculus", Interscience Publishers, Inc., New York, 1937.
23. Greenwood, I. A., J. V. Holdam and D. MacRae, "Electronic Instruments", V. 21, Massachusetts Institute of Technology Radiation Laboratory Series, McGraw-Hill, New York, 1948.
24. Jones, Paul: "Stability of Feedback Systems Using Dual Nyquist Diagrams", Trans. of the I. R. E., V. CT-1, No. 1, pp 35, March 1954.
25. Terman, F. E.: "Radio Engineer's Handbook", McGraw-Hill, New York, 1943.
26. Timoshenko, S.: "Vibration Problems in Engineering", D. Van Nostrand, New York, 1955.
27. Young, D.: "Vibration of Rectangular Plates by the Ritz Method", Jour. App. Mechanics, V. 17, No. 4, pp 448-53, December 1950.

## APPENDIX I

## PROOF OF SOME THEOREMS ON THE NODES OF EIGENVECTORS

Courant and Hilbert (Ref. 13, pg.31) have shown that the  $h$ -th eigenvalue of the equation

$$[K - \lambda M] x = 0 \quad (\text{AI-1})$$

may be characterized as follows: Minimize the quadratic form  $x^t K x$  under the normalizing condition  $x^t M x = 1$  and the  $h-1$  auxiliary constraints  $v_i^t M x = 0$ ;  $i = 1, 2, \dots, h-1$ ;  $h \leq n$ . The maximum value of  $x^t K x$  obtained under these conditions for all arbitrary vectors  $v_i$  is the  $h$ -th eigenvalue  $\lambda_h$ .

This idea may be used to prove the following general theorem:\*

Given the vibrating system characterized by the equation  $[K - \lambda M] x = 0$  for a domain  $G$  with arbitrary homogeneous boundary conditions; the nodes of the  $h$ -th eigenvector\*\*  $x_h$  divide the domain into no more than  $h$  subdomains. No assumptions are made about the number of independent variables. In particular, the eigenvector of the lowest mode has no nodes.

Assume for simplicity that  $G$  is a two dimensional domain, and that the  $h$ -th eigenvector  $x_h$ , divides it into more than

---

\* This is a paraphrase of a theorem proven in Ref. 13, pg.451 for the eigenvalue problem of a differential equation. The proof is the same except for minor modifications.

\*\* A node occurs on the spring connecting two masses which have displacements of opposite sign, or at a mass with zero displacement. Physically, in the first case, there is a point of the spring which does not move.

$h$  subdomains  $G_1, G_2, \dots, G_h, G_{h+1}, \dots$ . Define  $h$  vectors  $w_1, w_2, \dots, w_h$  which coincide with  $x_h$ , except for a normalizing factor, within their respective domains and are identically zero outside them. The  $w_i$  are normalized by the condition  $w_i^t M w_i = 1$ . Form a linear combination of the  $w_i$ 's;

$$\psi = c_1 w_1 + c_2 w_2 + \dots + c_h w_h \quad (\text{AI-2})$$

such that it also satisfies

$$\psi^t M \psi = c_1^2 + c_2^2 + \dots + c_h^2 = 1. \quad (\text{AI-3})$$

The  $h-1$  auxiliary constraints  $v_i^t K \psi = 0$ , taken with AI-3, completely specify the constants  $c_i$ . Using the system equation (AI-1) it is seen that

$$\psi^t K \psi = \lambda_h \psi^t M \psi = \lambda_h \quad (\text{AI-4})$$

Another theorem is needed before continuing:

If  $G'$  is any subdomain of  $G$  with the boundary condition  $x = 0$  on the non-common boundaries and any homogeneous conditions on the common boundaries, the  $h$ -th eigenvalue of  $G'$ ,  $\lambda'_h$ , is not less than  $\lambda_h$ , the  $h$ -th eigenvalue of the larger domain.

The proof lies in considering the effect on the system as the boundary of  $G'$  is deformed to match that of  $G$ :

i) the unstressed length of a spring may be made longer, thus making the system less stiff.

ii) a new mass may be added to the system.

Both of these effects operate to decrease (or at least not change) all eigenvalues.

Returning to the original theorem, consider the domain  $G' = G_1 + G_2 + \dots + G_h$ . Since  $\psi$  satisfies the system equation and all constraints and the condition  $\psi^t K \psi = \lambda_h$ , the  $h$ -th eigenvalue for this special domain must satisfy the maximum-minimum condition described above. In addition it must satisfy the last theorem, so that

$$\lambda'_h \leq \lambda_h \leq \lambda''_h,$$

and equality must hold. Then for every subdomain of  $G$  containing  $G'$  the  $h$ -th eigenvalue must be  $\lambda_h$ .

Designate by  $x'_h$  the  $h$ -th eigenvector for  $G'$  which is extended to the entire domain  $G$  by taking it to be zero outside  $G'$ . A suitable constant multiplier may be chosen to satisfy the normalizing condition  $x'^t_h M x'_h = 1$ . Then, by the maximum-minimum principle, since  $x'_h$  is a vector of the full domain

$$x'^t_h K x'_h \leq \lambda_1. \quad (\text{AI-5})$$

On the other hand

$$x'^t_h K x'_h = \lambda_h x'^t_h M x'_h = \lambda_h \quad (\text{AI-6})$$

These equations are clearly incompatible so that the assumption of more than  $h$  subdomains is incorrect.

Actually much more can be proved in the one dimensional case:

Given the vibrating system characterized by the equation  $[K - \lambda M] x = 0$  for a domain  $G$  with arbitrary homogeneous boundary conditions; the nodes of the  $h$ -th eigenvector divide the domain into exactly  $h$  subdomains.

Let  $a_1$  be the normalized eigenvector for the lowest eigenvalue,  $a_2$  that for the second eigenvalue, etc. Since  $M$  is positive definite and  $a_1$  has no nodes, each of the elements of the column vector  $M a_1$  is positive. By definition  $a_1^t M a_1 = 0$  so that  $a_1$  must change sign at least once within  $G$ . Applying this reasoning to the subdomains formed by the various eigenvectors, it is seen that of two eigenvectors with different numbers of nodes, the one with the least nodes has the lowest eigenvalue, for it must have at least one subdomain with more than one node of the other eigenvector. Then each eigenvector must have one more node than the previous one but not more than  $h-1$ . Since the first has no nodes the  $h$ -th must have  $h-1$ .